VIDEO DE-NOISING USING VECTOR ESTIMATION OF WAVELET COEFFICIENTS

by

Eesha Oaj

A thesis submitted to the faculty of Electrical Engineering Department, Military College of Signals, National University of Science and Technology, Rawalpindi in fulfillment of the requirements for the degree of MS in Electrical Engineering.

February 2017

ABSTRACT

Image de-noising based on wavelet can be extended to video de-noising by using it on each frame separately. By manipulating inter-frame correlations de-noising performance can be enhanced by using appropriate temporal filtering. Fixed temporal filtering may not give appropriate results due to their inability to deal with the variations of inter-frame correlations. Many adaptive temporal filtering methods for de-nosing in spatial domain exist, but they do not directly outspread in wavelet-based de-noising.

In scalar Hidden Markov Tree, prior state probabilities are plugged into algorithm to estimate conditional probability density function. Hidden Markov tree modeling vector extension in wavelet domain is proposed, that exploits the frame reliance of wavelet coefficients. This will estimate unknown parameters by using expectation maximization algorithm.

Experimental results reveal that the vector estimation of wavelet coefficients gives better de-noising performance as compared to existing techniques, in terms of quantitative and qualitative analysis.

DEDICATION

I dedicate this report to my parents, and my supervisor, Col. Dr. Imran Touqeer for their prayers and encouragement

ACKNOWLEDGMENT

I thank Allah who provided me with strength and caliber to bring this thesis work to its successful completion.

I am deeply obliged to my supervisor, Col. Dr. Imran Touqeer, for his guidance, unwavering support and confidence in me throughout the course of this thesis work. His time and efforts were very valuable. He contributed significantly in the thesis work and also imparted a lot of knowledge to me. I am also grateful to my Guidance and Evaluation Committee, Lt. Col. Dr. Adil Masood, and Lt. Col. Dr. Adnan Rashdi for dedicating their time and making contributions to this thesis work. I offer my regards and blessings to all of those who supported me in any respect during the completion of this work. Alongside that, I thank the university administration, for facilitating the progress of work at different phases, faculty members of MCS for polishing my knowledgebase, my university mates and friends.

Last but not the least; I am grateful to those people without whom I could never have accomplished my aim my family, especially my parents. I thank them all for their constant prayers and unfaltering support throughout this journey. May Allah bless them all with eternal happiness.

NOTATION

MSE	Mean Square Error
WGN	White Gaussian Noise
AWGN	Additive White Gaussian Noise
CWT	Continuous Wavelet Transform
DWT	Discrete Wavelet Transform
EM	Expectation Maximization
GMM	Gaussian Mixture Model
HMM	Hidden Markov Model
PDF	Probability Density Function
HMT	Hidden Markov Tree
PMF	Probability Mass Function
PSNR	Peak Signal to Noise Ratio
STFT	Short term Fourier Transform

IMM	Independent Mixture Model
MAP	Maximum aposteriori
CMF	Conjugate Mirror Filters
FFT	Fast Fourier Transform
IDWT	Inverse Discrete Wavelet Transform

Table of Contents

List of Figures

List of Tables

Ｃｈａｐｔｅｒ１

Introduction

Digital image processing has a broad spectrum of applications, and it has rapidly evolving fields with many theoretical as well as technological breakthroughs during the last decades. Generally speaking, there have been mainly two trends in the image processing research: one leads to the fundamental image representation and modeling techniques, and the other heads a variety of image processing applications. The two topics are so closely related and have greatly been stimulated by each other. Both of them benefit from the widespread use of computers with powerful computational capability, and the development of human life science, multimedia, and Internet technologies.

Edge preservation property of wavelet based frame de-noising has achieved a remarkable popularity in the last ten years. Through wavelet transform video frame can be divided into a sub band of lower frequency and multi scale high frequencies coefficients. Smooth areas correspond to small coefficients in high frequency sub band, while edges contain larger coefficients. Based on the states of wavelet coefficients which are small or large, edge preservation can be attained through different de-noising rules [1] – [4]. By using inter- scale [4] correlations, frame de-noising can considerably be enhanced. Frame resolution and improvement are major difficulties in image processing. Improvement of degraded frame through prior knowledge of degradation rule is the main purpose of restoration, while extraction of better video frame than original one is the main purpose of enhancement [1].

The principle purpose of restoration is to improve a corrupted image with the help of past information utilization regarding degradation rule while the goal of enhancement is to obtain a better image than the original one for a specific purpose

[1]. In brief, restoration is an objective process and enhancement is a subjective one. In both cases, image de-noising, sometimes called noise removal, plays an important role. De-noising is the procedure which removes the existing noise in an image and minimizes the loss of information in a clean image.

A problem that involves the estimation of clean images with the help of information obtained from conducting noisy observation is referred to as image de-noising. Wavelet transform can be regarded as an instrument that is used for processing of signals or images on statistical basis. Applications that includes prediction, synthesis, filtering, compression, classification, detection, estimation in real time could exploit the natural settings offered by the wavelet domain. When the statistical approach that is based on wavelets is adopted, the coefficients are regarded as arbitrary realizations and hence the distribution of theirs could be estimated with the models of probability [2][3]. The extraordinary characteristics that wavelet transforms possess resulted in the emergence of powerful methods of image/signal processing that only involves the wavelet coefficients to through basic scalar transformations. With the help of such new models, sophistication has been brought into the techniques of processing. These techniques cooperate with the nonlinear processing to give much higher performance than the existing methods of processing that are wavelet based.

1.1 Past research in the relevant area

A wide range of applications are based on the signal processing that is carried out statistically. De-noising based on wavelets and Hidden Markov tree model use all possible values of scaling coefficients.

Wavelet based de-noising decompose the image into multiscale coefficients of high and low frequency components. For video, it is extended to each video frame separately and then taking averages of all frames.

1.2 Thesis Statement/Synopsis

The wavelet coefficients in statistical processing of signals based on the wavelet, are modeled either as jointly or statistically independent Gaussian. Time consumption with these models impose constraints on their employment for real time applications such as Signal detection, signal compression, signal estimation, signal classification and De-noising of signals.

The main objective of this work is the development of a structure for vector estimating of the coefficients of wavelet, so that de-noising could be applied in a video signal. The vector tree model of Hidden Markov is deployed for pursuing the basic goal in the process. The resultant framework is capable of enabling the concise modeling of the wavelet coefficients collectively. Furthermore, the probability density functions could be obtained as a collection of two Gaussian distributions with zero mean.

1.3 Objective

The primary objective is to develop a model for video de-noising based on vector estimation of wavelet coefficients. This framework will allow extension of scalar model of HMT to vector HMT, which will estimate coefficients jointly over all the quad-tree. Maximization algorithm for efficient expectation has been applied in this model for the estimation of parameters.

1.4 Methodology used

Two steps are involved in this thesis.

- The development of a wavelet domain model constitutes the first step

    The step is started by focusing on the achievement of primary characteristics for wavelet transform. For acquiring the secondary properties, the extension of framework is carried out by utilizing the vector estimation of wavelet coefficients.

- The algorithm's development is contained by the second stage, which is performed via vector estimation of wavelet coefficients for achieving the signals de-noising.

1.5 Benefits

- The efficiency lies in the complexity of computation
- The reduced complexity in computation in the framework being proposed is likely to result in the efficiency for:
  - De-noising of Signal
  - Compression of Signal
  - Estimation of Signal
  - Detection of signals
  - Classification of Signal

1.6 Application areas

A widespread use of this practice could be found in the areas of:

- Interpretation and processing of spoken words in the signal processing of speech
- Widely used in imaging systems and Image Processing in digital cameras or computers
- Processing of videos for interpretation of pictures in motion
- The processing of signals obtained from sensors array
- For signal processing of audio on the signals that represents sound, for instance music or speech signals
- Also, use in Control Systems
- It also has application in Wireless Communications for instance: in equalization, filtering, demodulation and waveform generation.
- Also, used in the extraction of features from signals such as speech or image recognition
- For compression of Image, Video or Audio signals

1.7 Thesis outline

The following chapters are included in this thesis:

Chapter 1

    Basics of the topic are introduced in this chapter along with the scope, objective and problem statement of this work.

Chapter 2:

    In the second chapter, wavelet transform and wavelet basis are going to be introduced. Essential understanding of the methods deployed in the statistical signal processing along with its significance has to be given in this chapter.

Chapter 3

    The third chapter provides the description of vector estimation of wavelet coefficients used for video processing and de-noising. The framework of models along with the associated calculations is explained in this chapter.

Chapter 4

    The older filtering techniques that help in achieving the de-noising of signals and their comparison with our proposed technique are discussed in this chapter.

Chapter 5

    The results of experiment and simulations that aimed at achieving the de-noising of videos are included in this chapter.

Chapter 6

    In the light of previous chapter conclusions will be drawn in this chapter to provide recommendations on the future work.

CHAPTER 2:

INTRODUCTION TO WAVELETS

2.1. Wavelet

Disturbances in the form of periodic oscillations that goes through propagation is time and space, that mostly involves the transfer of energy along with it, is termed as a wave. Confinement and concentration of waves in space or time that becomes better suited for transient signal's analysis could be referred to as wavelets. Hence, it is mostly referred to as a confined variation of sound in one dimension or confinement of details varying within a two-dimensional image. So, wavelets could be utilized for numerous signal processing tasks, for instance image or sound enhancement, noise removal, edges detection and compression of signals. It could be considered as a mathematical function which could be used for the division of data with continuous time signals into three components of frequency. These are followings: -

- Rapidly changing parts of signal are of high frequency
- Low frequency slowly varying piece.
- The remaining part that remains unchanged has 0 frequency

The crucial notion in wavelets is examination in accordance with gage. A simplest method of imagining scale would include the use of piano's analogy. While talking about wavelets, representation in time-scale is usually referred to instead of representations in time-frequency. There exists a function ψ *for* each wavelet, which is termed as mother wavelet that could be represented as

$$\Psi_{i,j}(x) = \sqrt{2^i}\psi(2^i x - j), \qquad\qquad i,j = 0,\pm 1,...$$

The title of "mother wavelet" is given to it due to the type of function that it has to perform. Mother wavelet serves as a prototype that results in the generation of functions that further have to be utilized in the process of transformation. It has several levels of offspring signals such as children, grandchildren and so on. The original signal's size is the only thing that

constraints mother signals as it is allowed to produce only *n* number of generations for every signal with 2^n number of samples.

A scaling function φ(*x*) which is also referred to father wavelet sometimes exists for any mother ψ(*x*). Translations and dilations of are denoted as $φ_{i,j}$. Translation could be located for the interval as it is examined for the signal shift. Hence, scale is the contraction or dilation. For instance, the figure 3.6 (a) and 3.6 (b) illustrate the mother wavelet ψ and scaling wavelet φ respectively. Apart from this, the below mentioned equation described in detail the single dimensional wavelet transform.

$$W_f(a,b) = Z f(t)ψ(at + b)dt$$

2.2. Applications of wavelet

Fourier analysis had been performing well in particular cases for a very long time, yet there always had a need existing for more suitable functions as compared to sine and cosine. The information obtained from physical phenomena had mostly been containing sharp spikes that couldn't be precisely analyzed with the help of sine and cosine basis. Non-local nature and its stretching to infinity had been indicated by the definition. Hence, when it comes to the approximation of choppy signals, the performance of Fourier transform is very insufficient. More compressive discussion of this will be conducted in the section 3.2 of the next chapter.

This is the requirement in the development of a number of applications from real-world. Therefore, wavelet theory is utilized for developing a number of disciplines. These are the following examples: -

- In Image Processing compression standards of JPEG 2000 have been there for a very long time. Compression standards for fingerprints in the Federal Bureau of Investigation (FBI) of US also find the use if wavelet theory [5] [6]

- Earthquake Prediction is made by using wavelet theory in Seismic Geology

- Solar Cycle Complexity, Determination of Coronal Plasma, Tidal Tails Around Stellar Systems are the areas of Astrophysics and Astronomy that could make use of the wavelet theory.

- Central England Temperature, Tropical Convection, The El Niño Southern Oscillation (ENSO) [8] are the areas where wavelet theory finds its applications in geophysics [7-10].
- Ship Roll,Tide Forecasting, Underwater Sonar are the areas where ocean engineering can find the applications of wavelet theory
- Detecting Edges of Filopodia is an example of Human vision application [11-12]

The wavelets' tendency for analyzing the information in time-frequency domain illustrates that all of these applications would need the implementation of wavelet theory to them. Therefore, wavelet transform fulfills the needs where Fourier transform would not be successful.

2.3 Fourier Transform

In the area of signal processing, an innovative and leading edge influence has been experienced with the development of wavelet. A signals' transformation is merely another form of its illustration. The content of information contained in a signal remains the same. The representation of a Fourier transform in the form of cosine signals could be taken as a simplest example. Hence the similarities and dissimilarities are explained in the next chapter with great details.

Fourier Transform (FT) has been well established method of providing frequency domain representation of a signal. Joseph Fourier (French mathematician) claimed that complex periodic exponential functions could be used for showing any periodic function as their infinite sum.

Therefore, Fourier Transform revealed extent to which each signal has the contribution from different frequencies. Theoretically speaking, Fourier transform when compared with the wavelet transforms, sine and cosine wave could be considered analogous to the parent wavelet due to the fact that basis functions of Fourier transform are the sine waves of varying frequencies phases and amplitudes. Fourier transform is defined as follow:

$$X(f) = \int_{-\infty}^{\infty} x(t)e^{i2\pi ft} \, dt$$

Here f= frequency, t= time domain and *X (f)* denotes the representation of signal in frequency domain. It should be noted that the signal that is desired to be decomposed into its frequency components in continuous spectrum is represented as x(*t*).

Fourier transform is referred to as Discrete Fourier transform when is required to meet the need of operating on sampled and distinct values of finite duration signal. X_k is computed from x_n by the Discrete Fourier transform. Its equation is written as follow:

$$X_k = \frac{1}{N} \sum_{n=0}^{N-1} x_n e^{\frac{-2\pi i}{N} kn} \quad k = 1, 2, ... N - 1$$

Phase and amplitude for various sine components from the x_n which is the input signals is represented by X_k the complex number. The Fourier analysis of discrete time functions in time domain is a DFT transform. Algorithms of Fast Fourier transform is utilized for the determination of values for Discrete Fourier transform that is a very economical, fast and efficient algorithm for carrying out the required calculations of DFT along with its inverse.

A signal going through resolution into its frequency elements could also be constituted back from the constituent elements into its original form by making use of FT equation which could be expressed as follow:

$$x(t) = \int_{-\infty}^{\infty} X(f) e^{i2\pi ft} \, df$$

X(f) could be used for the determination of signal's amplitude. Phase of the signal represented by is represented in the *e*'s superscript part as *iφ(f)*. Hence, exponential term could be represented by a combination of a cos and a sine term, where the cosine of *2πft* refers to the real and its sine refers to the imaginary part. Equation for Inverse of Discrete Fourier Transform is expressed as follow:

The Inverse Discrete $\frac{k}{N}$ Fourier Transform represents the computation of as summation of N number of products between DFT coefficients X_k and sinusoidal terms. *k*/N is the per cycle frequency.

In a nut shell, whether it's discrete or not, FT remains an infinite distended cosine terms' combination each of which shows the presence of certain frequency along with its contribution to the original signal. For each of the frequencies, there exists possibilities as follow:

- If for any values of frequencies, the integration gives out a zero result, the frequencies do not exist as components in the signal.
- If the integration for certain frequencies comes out to be very small value as compared to others, then the contribution to signal from such 'f' is very minor.
- Similarly, if the integration result is a very large value, the spectral portion of the signal is very prominent at those frequencies.

Since, in the equation of transformation, the integral is taken over time, the left side of the equation is function of 'f'. Hence, it calculates the integral for all values of 'f' one by one.

Now, note that the integration in the transformation equation is over time. The left-hand side is a function of frequency. Therefore, the integral is calculated for every value of f.

In the following figure equation of $x(t) = \sin(2\pi50t) + \sin(2\pi120t)$ is represented in the form of plot. If we examine this equation, we would see that it has two frequency components such as 120 and 50 Hz. Since at a certain time instant, this signal has frequencies of 120 and 50 Hz, it could be referred to as a stationary signal.
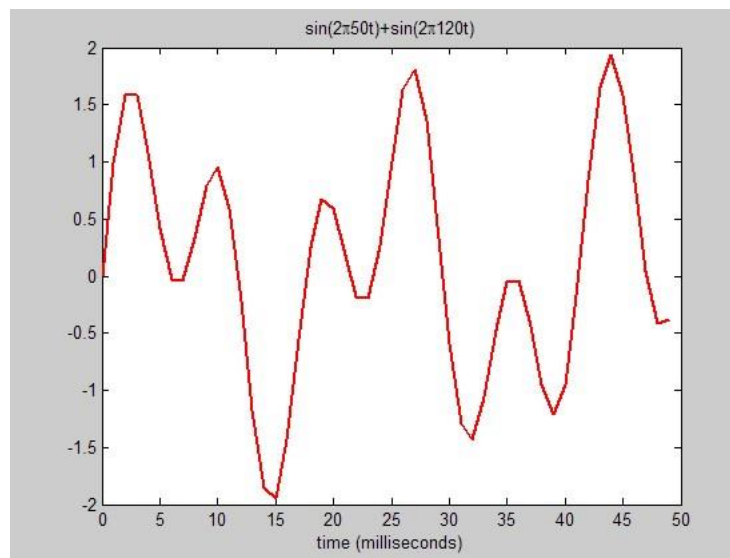

Figure: 2.1 Example of a stationary signal with two frequency components

The Fourier transform of above signal is shown in the figure 2.2. In this figure the approximated value of frequency is shown to be 125Hz at maximum that should have theoretically approaching to infinity. However, the two maximum points have been agreeing on the distinction of frequency components.

10
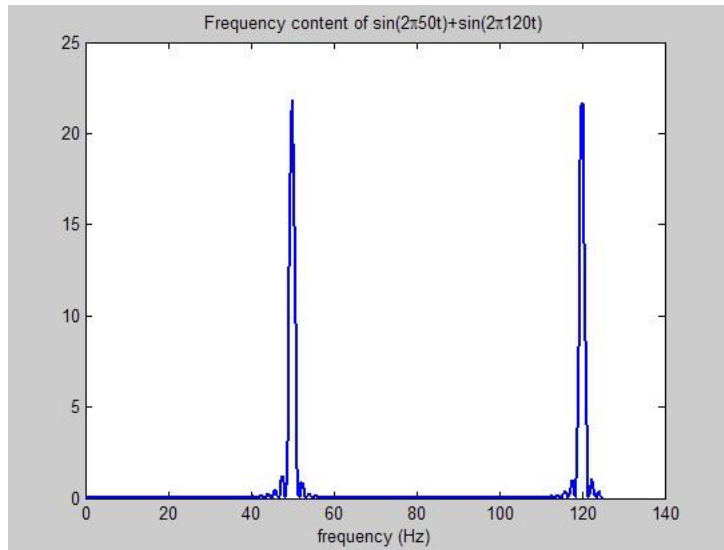
Figure: 2.2 FT ($X(f)$) of signal

Identical signal $x(t) = sin\left(2\pi\left(f_0 + \frac{k}{2}t\right)t\right)$ has been shown in the fig 2.3 with the addition of chirp into previous signal. The frequencies of this signal are similar to those of the previous one but it lacks the periodicity as the previous one. Occurrences of these frequencies at different instances can be observed here. When a Fourier transform is applied on this new signal with addition of Chirp, it appears to be very identical to that of 2.1. Time and frequency domain analysis for these two identical signals is very important. As, the frequency components could see at varying positions in the time domain, the information in time domain makes the two of them less identical. It could be observed in a very straight forward manner yet it also could be seen that FT may fail to differentiate between the two signals due to the sameness of their frequency components despite the need for the signs to be aided. Fourier transform would perceive both of the signals to be similar due to the recurrence of the same signal constituents. Hence, it could be stated that Fourier transform is inadequate to account for the non-stationary signals as it is incapable of flying to capture such signals that may be varying in their spectra in long term. If the interest of analysis lies merely in the understanding of frequency components the Fourier transform tool may be the desired instrument for utilization.

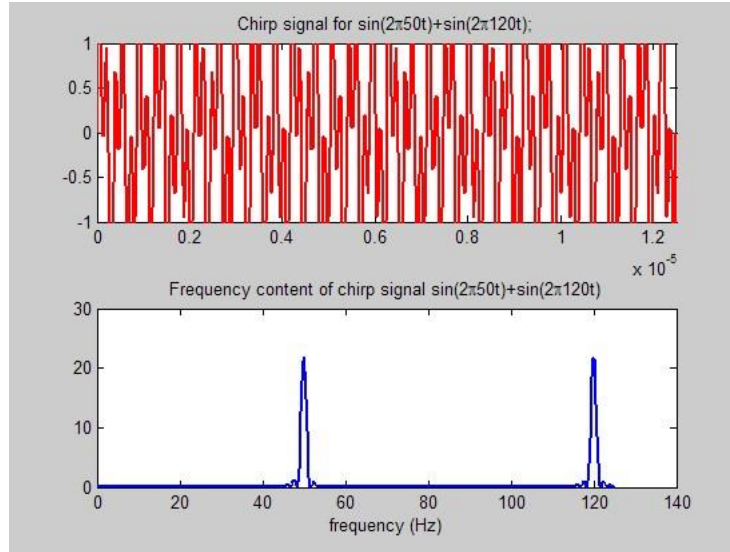**Figure: 2.3 The signal *x*(*t*) = sin(2π50*t*) + sin(2π120*t*)**

2.3.1 Comparison between Wavelet and Fourier

Fourier and Wavelet transform share a number of characteristics along with variations. Both of the algorithms DWT and FFT are linear ones. For each n sample signal, both of these transforms decompose it into $\log_2 n$ segments of bits for varying lengths.

There are some similarities between the FT and the WT. Both the fast Fourier transform (FFT) and the discrete wavelet transform (DWT) are linear algorithms. For a signal with *n* samples, each transform decomposes a signal into bits that hold numerous for different lengths. An example of discrete wavelet transform could be used for elaborating this, in which upon application to the signal, fragmentation is resulted into details and approximation of the signal where each part is half of the original signal. There are two important parts associated with the proper illustration are held by the signal subjected to the Fast Fourier transform, the recent one of which possess greater coverage over the Nyquist frequencies.

A distinctive characteristic of WT lies in its ability of varying window. Basis functions with longer length provide in depth analysis of frequencies. For the discontinuities of signals, the short basis is more appropriate. Such comprehensiveness is provided by the WTs.

In a nutshell, there are several disadvantages associated with the Fourier Transform:

- It has to offer a wider illustration and doesn't show local information
- Majority of the naturally existing signals do not simply contain sinusoidal combination

12

- The applicability of FT is limited to LTI systems and stationary signals
- Performance of FT is very poor for changes with time in frequencies
- The compact support that WT can offer is missing in Fourier series. Due to the compactness of interval, both of end points are contained in it. For instance, usually the interval is written in the form of square brackets to show compactness.

Hence, the wavelets are more appropriate for time-varying signals along with the transient ones and their energy is concentrated in time. Transient signals that are having finite duration are non-stationary in nature and any natural phenomena would include signals like these. Concentration of human sensory systems in transient could be found in several examples such as heartbeat ECG patterns having abnormal electrocardiogram, a part of sentence being spoken and an edgy instant in an image. So, WT fits to the majority of applications due to its ability of handling real life signals that are time varying.

2.3.2 Rationale behind Wavelets

A number of fundamental explanations could be behind the utilization of wavelets. There could be varying number of reasons among varying nature of applications for choosing wavelet over other instruments. For instance, some of WT may be performing in such a wat that they divide signals into components that are significance in space and time meanwhile keeping the contribution low. Such characteristic of wavelet makes it to be significant in applications that involve data compression, edge detection and noise removal.

Usually wavelets are useful in exploiting the signals for more information that may not be readily obtainable from the raw signals. Meanwhile, a signal's transform just remains another form of its representation. No changes in the signals content being presented are made by a transform.

Wavelets are appropriate waves for transient signals' analysis in localized manner with their energies concentrated in space and time. For instance, wavelets are utilized for performing the forecasting of tides. As the oceans ripples are transient in nature, wavelet has been chosen to the appropriate choice.

Images are efficiently broken down into details and approximation with the help of wavelets for watermarking. Lower and higher resolution bandwidths could be separated in an

effective manner for embedding water marks into the bands in such a way that they become barely visible to human sight.

Embedded information into image could be analyzed in terms of its time-frequency content with the aid of multiresolution. Its interpretation may be questioned at this point. Hence, the details are made available to the algorithm of water marking. For hiding the water mark from human sight, exploitation of multiresolution could be approached. The details could be used for concealing the information. The information being hidden is supposed to have robustness as approximated information has lesser likelihood of getting an impact from the modification of image, for instance from the addition of noise or compression. Decomposition of complex patterns and information into constituent forms is the ability possessed by wavelet transform. It also keeps track of its record.

Hence, WT finds its implementation in various other applications too. Lossless construction during which the original data could be retained without having to keep the image watermark's original copy could be accomplished by the utilization of wavelets in signal processing.

2.4   Types of Wavelet

For overcoming the problem of resolution continuous WT had been developed. CWT is utilized for dividing the functions that are continuous time into wavelet. The process of implementation is same as that of SFTF. Hence, in place of multiplying it with a window function, it is multiplied with a mother wavelet. The CWT for a square continuous signal with τ as its translational value is expressed as follow:

$$X_w(\tau, s) = \frac{1}{\sqrt{s}} \int_{-\infty}^{\infty} x(t)\psi^* \left(\frac{t - \tau}{s} \right) dt$$

S represents scale, $\psi(t)$ represents mother wavelet and * denotes the complex conjugate operation. The fundamental aim of the "mother wavelet is to produce function source for generating "daughter wavelets" that have gone through simple scaling and translation of the parent signals. Meanwhile the inverse CWT could be utilized for the generation of original signal *x(t)* as follow:

$$x(t) = \int_0^\infty \int_{-\infty}^\infty \frac{1}{\tau^2} X_w(\tau, s) \frac{1}{\sqrt{|\tau|}} \phi\left(\frac{t-s}{\tau}\right) db \, d\tau$$

There are two important examples of CWT like Mexican hat and Morlet wavelet that are presented in the 2.4 (a) and (b). It's the shape of mother wavelet that gives its name to the Mexican Hat wavelet.
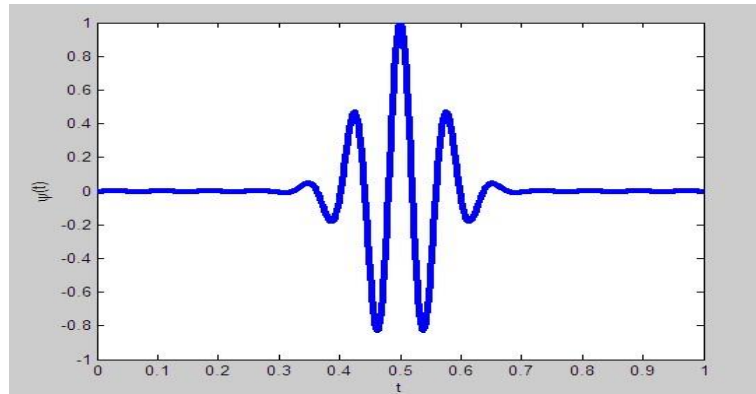
Figure: 2.4 (a) The Morlet mother wavelet ($\psi(t)$)
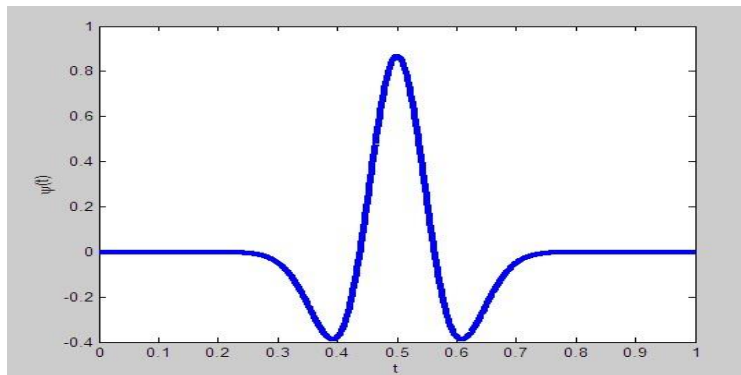
Figure: 2.4 (b) The mexican hat mother wavelet ($\varphi(t)$)

No functions of scaling as the mother wavelet are present in these continuous wavelet transforms. Hence CWT is resulted when set of functions that mother wavelet generates convolve with the input sequence. FFT could be used for the computation of convolution. A function of real value is obtained as an outcomes $X_w(a,b)$, meanwhile mother wavelet remains in the complex form. A CWT is transformed into complex form by the mother wavelet. The function of CWT is clearly illustrated in the fig 2.4. $|X_w(a,b)|^2$ shows its power spectrum.

15
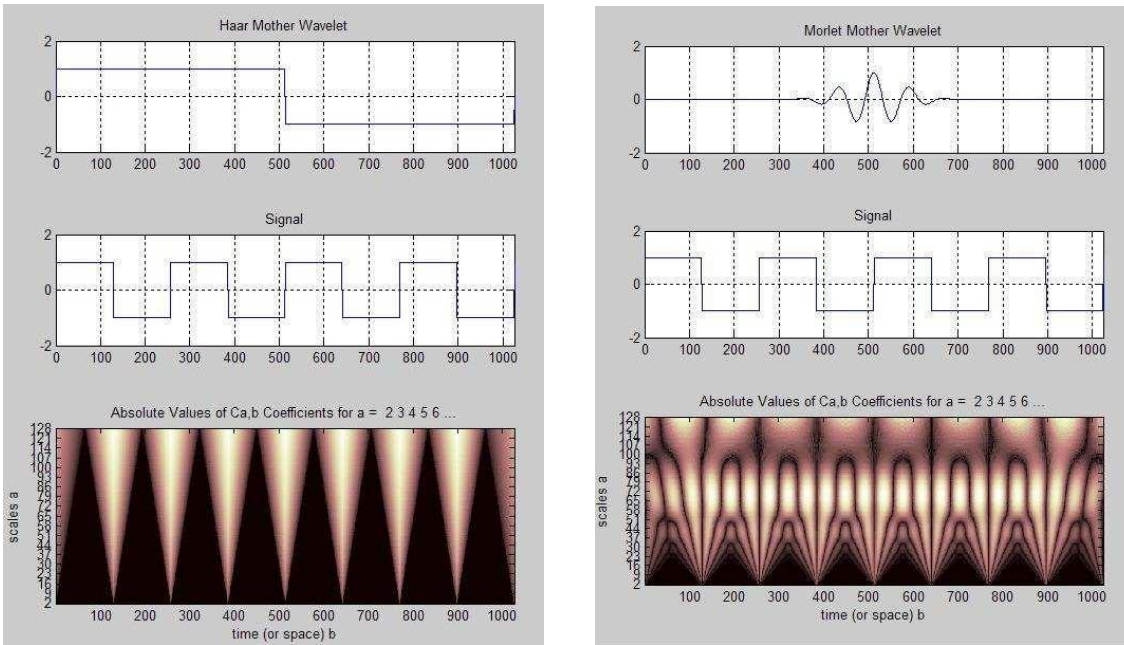
Figure: 2.5 CWT Interpretation of a Square Signal
(a) Haar CWT Interpretation of Square Signal   (b) Morlet CWT Interpretation of Square Signal

2.5 Haar Wavelet

In 1910, the idea of wavelets was introduced by Alfred Haar in his thesis but he did not use the name of wavelets. A Haar wavelet has resemblance with the step function and has discontinuity in it as depicted in the fig 2.6.
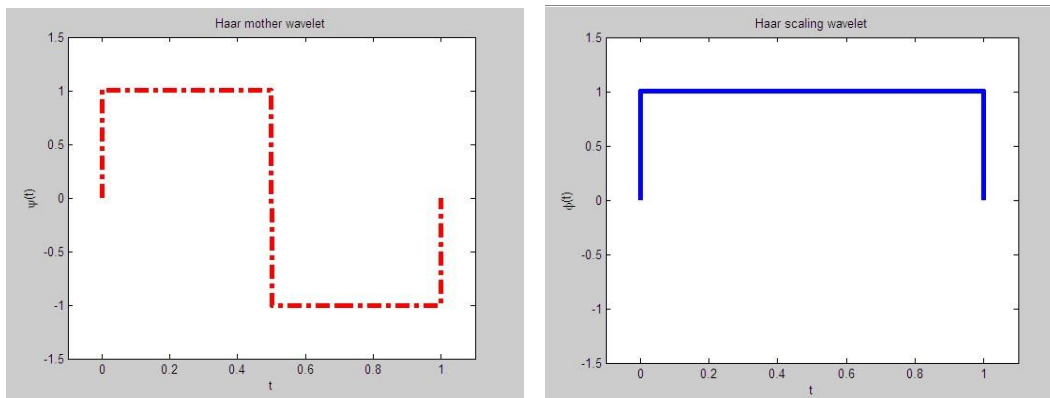
Figure: 2.6 The Haar wavelets
(a) The Haar mother wavelet ($\psi(t)$)   (b) The Haar scaling wavelet ($\varphi(t)$)

An interval of a signal says (0,1) can be divided into sub intervals for example (0,1/2) and (1/2,1). The division of intervals is aided by two functions. Such intervals could also be further subdivided by evenly division of portions such as $(0, \frac{1}{4})$ to $(\frac{1}{4}, \frac{2}{4})$, $(\frac{2}{4}, \frac{3}{4})$ and $(\frac{3}{4}, 1)$. For a large sized signal, even separation between intervals could be introduced over and over again. A particular scale or resolution is represented by each iteration. The function of mother wavelet for Haar is expressed as:

$$\psi(t) = \begin{cases} 1 & 0 \le t < \frac{1}{2} \\ -1 & \frac{1}{2} \le t < 1 \\ 0 & \text{otherwise,} \end{cases}$$

In the fig 2.7, a certain number of samples 'n' has been taken after every $\pi/5$ period and boxes in the figure is used for indicating it. The original signal is represented by line which is dashed and the samples have been taken from an overall interval of ($-\pi$ to $6\pi/5$).

A discrete signal is decomposed by the Haar transform into two sub-signals, each of which possess ½ of the original signal's length. One half shows the original signal is being approximated whereas the other half shows change or detail 'd' in spectrum. Frequency components makes the frequency spectrum of a signal.
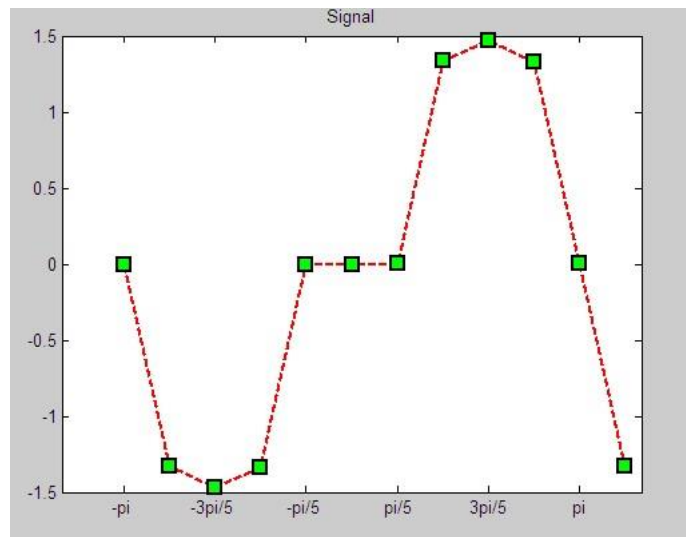
Figure: 2.7 The signal *f*(*x*) = tan(sin(*x*)) − sin(tan(*x*)) with 12 samples

17

Average and difference is performed by Haar transform on every set of details and approximation when are being produced. After that a shift of two values takes place in the algorithm and evaluation of other difference and average is applied on the pair.

It is shown in the figure that g(x) produces almost 1024 values of sample and the insert the graph over (0,1). In the given scenario, time is corresponded on the horizontal axis and amplitude is represented alongside the vertical one. It could be noted that the values along time axis have been dilated and shifted by half after staying up precise between 0 and .5.

Figure: 2.8 (a) The signal $x^2(1-x)^4 \cos 32\pi x$

Figure: 2.8 (b) Haar Transform 1 Level
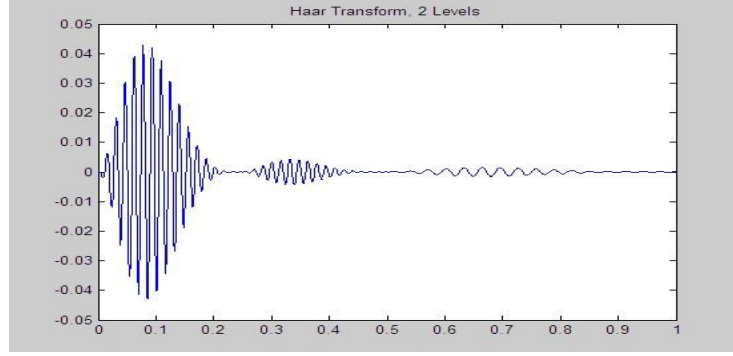
Figure: 2.8 (c) Haar Transform 2 Levels

It is shown in the figure 2.8 that for noise, ridding signals and compacting signals make use of Haar transform. The embedding of water mark into least visible portion is important in the watermarking applications. A spatial dimension may be assumed to be along the horizontal axis meanwhile the vertical scale may be showing the measuring intensity for every location sound. Then again, the similar kind of function could be representi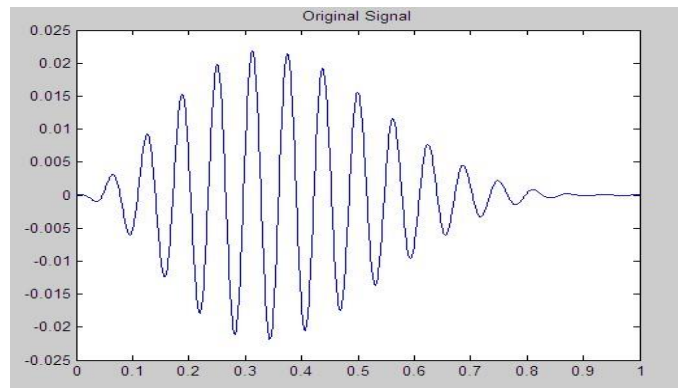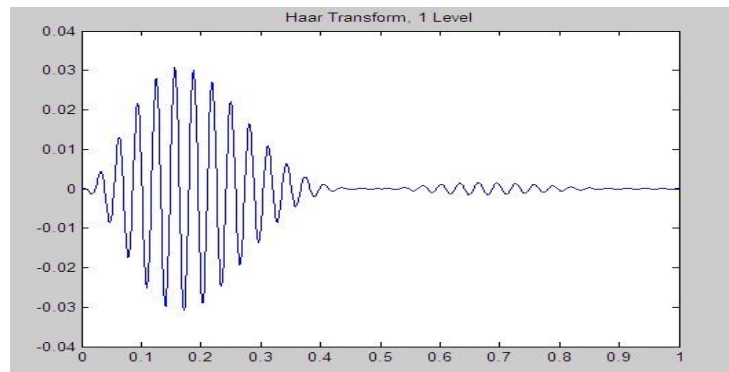ng the intensity of light in photographs. Haar transform of the function is shown in the fig 2.8 (b). Hence mathematical representation cam often leads to expressing varying signals along with their reconstruction and decomposition being applied to different kind of situations. For generating approximation, the following equation is followed:

$$a_N = \left(\frac{s_{2N} + s_{2N-1}}{2} \right) \sqrt{2}$$

$N = \{1...\frac{n}{2}\}$ is utilized. For computation of detail 'd'

$$d_N = \left(\frac{s_{2N-1} - s_{2N}}{2} \right) \sqrt{2}$$

for $N = \{1...\frac{n}{2}\}$ is utilized. Hence, approximation and detail signals as shown in the expressions above, are produced by Haar wavelet each of which is half of the original signal. One of them is the sum and other is difference of two adjacent values in the original signal divided each by '2' and then multiplied by the square root of '2'.

$s = \{4, -2, 3, 7\}$ which is a simple signal can go through Haar transform and gives out following:

$$s = \left(\frac{a_1 + d_1}{\sqrt{2}}, \frac{a_1 - d_1}{\sqrt{2}}, ..., \frac{a_N + d_N}{\sqrt{2}}, \frac{a_N - d_N}{\sqrt{2}} \right)$$

Previously obtained *a* and *d* are used to get:

$$s = \frac{\sqrt{2}+3\sqrt{2}}{\sqrt{2}}, \frac{\sqrt{2}-3\sqrt{2}}{\sqrt{2}}, \frac{5\sqrt{2}+(-2\sqrt{2})}{\sqrt{2}}, \frac{5\sqrt{2}-(-2\sqrt{2})}{\sqrt{2}}$$

Which provides us the perfect reconstruction of signal as:

$s = \{4, -2, 3, 7\}$.
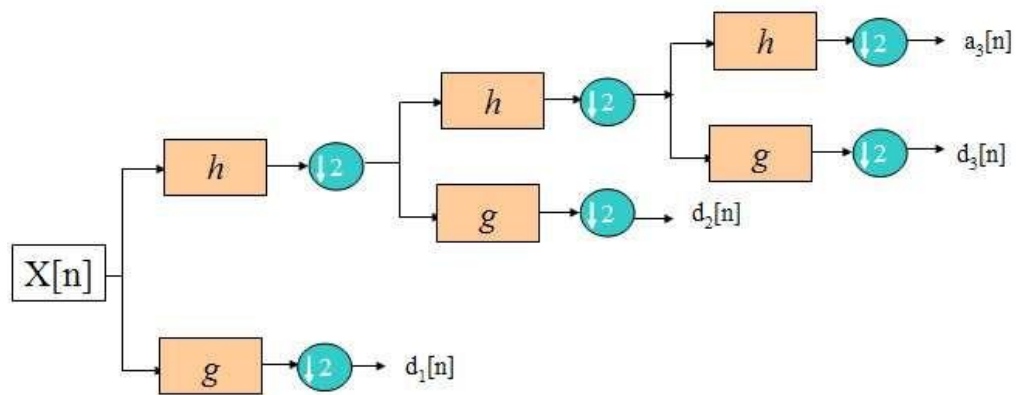
Figure: 2.9 1- Dimensional Discrete Wavelet Transform analysis or decomposition tree
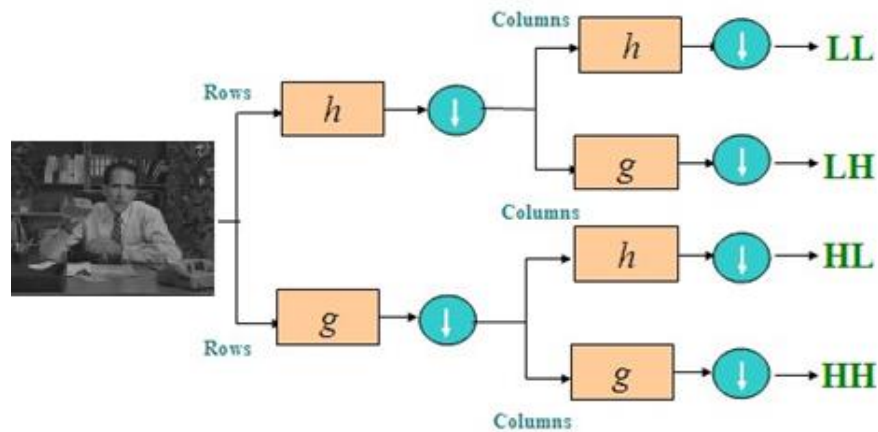
Figure: 2.10 2-Dimensional Discrete Wavelet Transform decomposition or analysis tree

2.5.1 Reconstruction

Discrete wavelet transform could be utilized for the decomposition as well as analysis of the signals. Moreover, no piece of information is subjected to loss in the whole process. Hence the components that have gone through transform are very likely to reassemble at the end of process for generating the original signal out of them. Such opposite phenomena of decomposition are referred to as synthesis or reconstruction of the original signal. The filters of finite impulse responses are utilized in this process and relation between them is kept so that a criterion of perfection is met at reconstruction. Aliasing is efficiently removed by such filters and the need to scale is eliminated along with it. To embed water marks, such criteria proves to be very important in meeting the required criteria's. The ability to have perfect reconstruction at the end is needed to be possessed in this application so that reconstruction of signals could be followed.

Resemblance exist between the original and approximation part. The addition of content in high frequency leads to the actual starting point. Such operation is known as Inverse DWT and shown in the figure as follow:
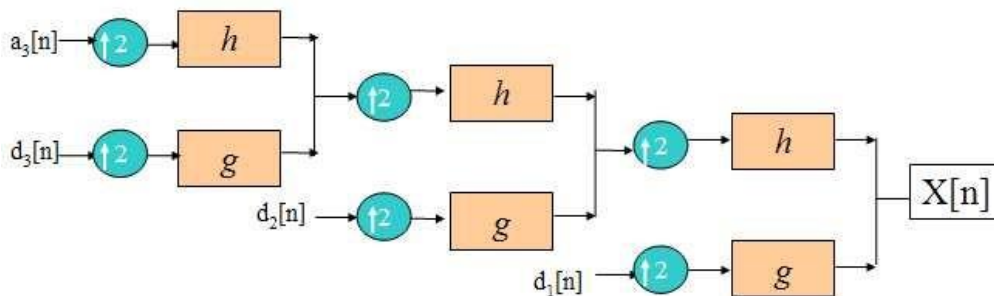
Figure: 2.11 1-D DWT synthesis or reconstruction tree
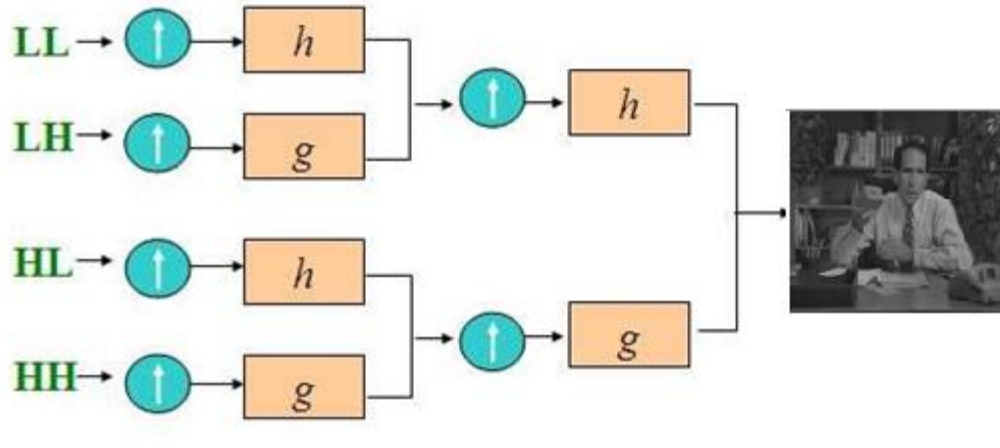
Figure: 2.12

Thus, the input vector got transformed into $\{6, -4, \frac{6}{\sqrt{2}}, \frac{-4}{\sqrt{2}}\}$. Four vector basis can be used for the reconstruction of the original 2-Dimensional DWT tree vector input of reconstruction or synthesis.

$$6 \cdot \{\tfrac{1}{2}, \tfrac{1}{2}, \tfrac{1}{2}, \tfrac{1}{2}\} = \{3, 3, 3, 3\}$$

$$-4 \cdot \{\tfrac{1}{2}, \tfrac{1}{2}, \tfrac{-1}{2}, \tfrac{-1}{2}\} = \{-2, -2, 2, 2\}$$

$$\tfrac{6}{\sqrt{2}} \cdot \{\tfrac{1}{\sqrt{2}}, \tfrac{-1}{\sqrt{2}}, 0, 0\} = \{3, -3, 0, 0\}$$

$$\tfrac{-4}{\sqrt{2}} \cdot \{0, 0, \tfrac{1}{\sqrt{2}}, \tfrac{-1}{\sqrt{2}}\} = \{0, 0, -2, 2\} \text{ Addition of receiving vectors } s = \{4, -2, 3, 7\}$$

Haar wavelets' concept for a given simple can be extended for n instances of information. Wavelet basis in the simple most for ate ($\{\tfrac{1}{\sqrt{2}}, \tfrac{1}{\sqrt{2}}\}$) and ($\{\tfrac{1}{\sqrt{2}}, \tfrac{-1}{\sqrt{2}}\}$). They can be utilized for the determination of single level Haar and signals that would scale.

There are a number of leading advantages possessed by the Haar transform. For instance, they are simpler, faster and efficient in terms of memory because it doesn't make use of temporary memory for its calculations. Furthermore, with Haar transform the exact signal without loss of any content in it could be reconstructed through the inverse of Haar transform and the losslessness needed for certain kind of applications becomes available owing to the characteristics of Haar transform in the signal processing.

2.5.2 2-Dimesional Wavelet Transform

Extension of the one-dimensional wavelet transform into two dimensional wavelets is easy to perform. Examples of two dimensional signals may include geographical measurements, scatter plots and photograph. The two-dimensional data would require to be operating on the input matrix and not just an input vector. For the transformation of input matrix for two-dimensional signal, the 1-dimensional transform has to be applied on each row. After taking the resultant value, the transform of 1-D type is also applied on the columns of matrix. Hence a final transformed form of matrix could be obtained with the help of 1-D transform. Such transformation finds its application in the area of image compression.

The rows of matrix can be filtered for carrying out 2-D transform to obtain two halves sized of the original signal's sub images. The heights remain same to the original but the width varies for the sub signals. The filtering of the sub images is then performed by making them pass through high and low pass filter alongside the columns. Such process leads to the generation of further sub images and hence eventually results in the four total sub images of the original signal. So, the process is known as analysis or decomposition. The resulted images are labeled from octave which is an iteration being named of the Discrete wavelet transform as diagonal HH, vertical horizontal HL, horizontal LH and approximation details LL in accordance with the filters that have been generating each of these sub images.

Two-dimensional DWT decomposition of signal is shown in the fig. 2.13. The upper left side of the image represents the approximation that is similar to the original one whereas the rest of three portions are showing the detail portion.
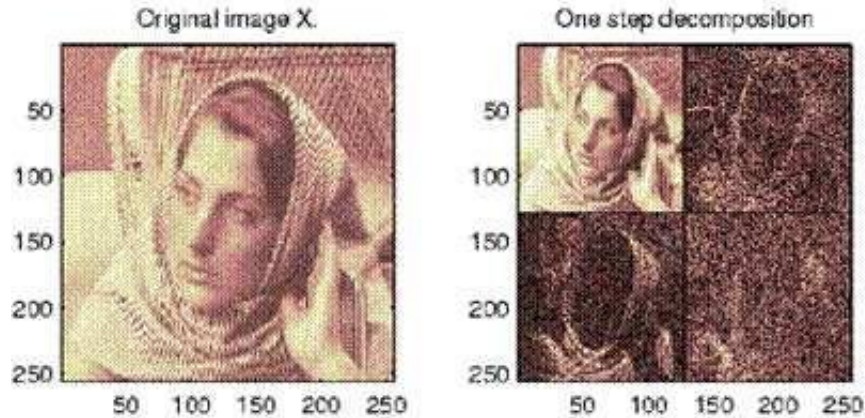
Figure:2.13 using the DWT for Barbara

For doing the two-dimensional WT, separable method could be followed such as by applying the transform separately for horizontal and vertical configuration. For the accomplishment of single dimensional Discrete Wavelet transform, single dimensional signal is broken in to two parts each of which is made to pass through each of high pass and low pass filter. Each of these filters corresponds to wavelet function and scaling function respectively. Filtering is one of the fundamental signal processing phenomena that convolves the single dimensional signal's input sequence with a set of its coefficients. The following expression shows two sequences being convolved:

$$output[n] = \sum_{m=0}^{M-1} input[n-m] \times coefficient[m]$$
.

Summation and multiplication could be utilized for carrying out these computations. An image is separated by Discrete Wavelet transform into its four sub images as discussed before. HL indicates that HP filter has been utilized along the rows whereas LP filter along the column. It has been shown in the fig 3.10. For representing the LP g is used in the figure whereas h is used for the HP filter. In addition to this, the details have been illustrated in the fig.2,13. Hence, the HP and LP filters for WT certainly decomposes the signal into rapidly varying, discontinue HP and same LP sub signals.

The slowly varying signal's characteristics are possessed by the channel with LP filter. Meanwhile the quickly varying portion is kept in the HP part of the channel. So, it is possible to

embed the watermarks of higher energy into regions that are subjected lesser to visibility by human sight. For instance, in the current situation, HH, HL and LH are high resolution bands of frequencies. The watermark could be made more robust by embedding into these regions while keeping the impact on quality to a very low or negligible level.

A question may arise here challenging the fact that image being approximated and recursive application of DWT for multiple times could be followed or not. Multiresolution involves the process of considering LL of one LL and by making this sub image to go through other construction of filter analysis. This could be iterated over and over again with LL. Each octaves detail is $1/4^{th}$ of the previous one. This is illustrated in the following figure.
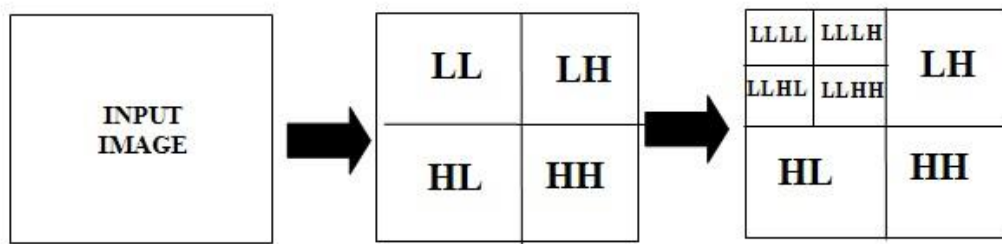
Figure: 2.14 Analysis or decomposition hierarchy for 2-Dimensional DWT

Discrete wavelet transform is an analysis at multi-scales that can be utilized for aiding the algorithm of water marking. The initial calculation is utilized as image 'seed' for recursive application of Discrete wavelet transform for as many times as needed to explore all the desired areas.

Two dimensional wavelets are needed in the image processing application. Therefore, this hurdle scales down for the two-dimensional filter's designing.

Separable filters are one of the classes that are capable of getting designed in accordance with their single dimensional equivalents. These are usually used for facilitating the explanations associated with the process. Alternatively, the filters of non-separable class provide the similar outcomes. Hence, the multiresolution analysis theories along with wavelets could be subjected to higher dimension generalization. In reality, the typical wavelet or 2-D scaling function choice is resulted from the product of two 1-D functions.

On the other hand, the non-separable filters give the same results. Therefore, the theories of multiresolution analysis and wavelets can be generalized to higher dimensions. In practice the typical choice for a two-dimensional scaling function or wavelet is a product of two one-dimensional functions such as $\varphi(x,y) = \varphi(x)\varphi(y)$. The following form is assumed for the dilation:

$$\varphi(x,y) = 2 \text{X} h(k,l)\varphi(2x - k, 2y - l)$$

$$k,l$$

As the dilation equation is satisfied by both of $\varphi(x)$ and $\varphi(y)$, wavelets could be constructed in an analogous manner. Yet, in place of single wavelet function, there would be now three of them.

$$\varphi^{(I)}(x,y) = \varphi(x)\psi(y)$$

$$\varphi^{(II)}(x,y) = \psi(y)\varphi(x) \quad \varphi^{(III)}(x,y) = \psi(y)\psi(x)$$

The conforming equations of dilation can be expressed as:

$$output[n] = \sum_{m=0}^{M-1} input[n-m] \times coefficient[m]$$

.

$$\varphi^{(I)}(x,y) = 2\text{X}g^{(I)}(k,l)\varphi(2x - k, 2y - l)$$

$$k,l$$

$$\varphi^{(II)}(x,y) = 2\text{X}g^{(II)}(k,l)\varphi(2x - k, 2y - l)$$

$$k,l$$

$$\varphi^{(III)}(x,y) = 2\text{X}g^{(III)}(k,l)\varphi(2x - k, 2y - l)$$

$$k,l$$

here $g^{(III)}(k,l) = g(k)g(l)$, $g^{(II)}(k,l) = g(k)h(l)$, and $g^{(I)}(k,l) = h(k)g(l)$

It should be noted that the principals followed by the single dimensional wavelets are retained in the world of two dimensional wavelets. For instance, the values of lower frequencies are retained by the details, when the high frequency values are contained in the approximation image. The summation of all rows or columns energies give rise to the energy of two-dimensional image. After the application of WT along all rows, the energy of original image is

retained by each row to 2nd octave. The next octaves also retain the same amount of energy and the energy is retained throughout the process.

2.6   Families of Wavelets

We have option to choose wavelet while using the discrete wavelet transform. Change could be brought into wavelet by bringing changes in the filter coefficients. Therefore, this research is focused on the discovery of the most appropriate ways of choosing the family of wavelets when approaching the use of Discrete wavelet transform in watermarking application.

A significant amount of contribution has been experienced by the area of wavelets from Daubechies. Details and approximation are produced differently by wavelets and scaling signals in Daubechies WT. The figure 2.15 has shown the four coefficient Daubechies mother wavelet and scaling wavelet. Four values of single dimension signals are contained by the scaling filters of Daubechie:

$$\alpha_1 = \frac{1+\sqrt{3}}{4\sqrt{2}}, \quad \alpha_2 = \frac{3+\sqrt{3}}{4\sqrt{2}}, \quad \alpha_3 = \frac{3-\sqrt{3}}{4\sqrt{2}}, \quad \alpha_4 = \frac{1-\sqrt{3}}{4\sqrt{2}}$$

The wavelet values for these single dimension signals are:

$$\beta_1 = \frac{1-\sqrt{3}}{4\sqrt{2}}, \quad \beta_2 = \frac{-3+\sqrt{3}}{4\sqrt{2}}, \quad \beta_3 = \frac{3+\sqrt{3}}{4\sqrt{2}}, \quad \beta_4 = \frac{-1-\sqrt{3}}{4\sqrt{2}}$$

Here $\beta_1 = \alpha_4$, $\beta_2 = -\alpha_3$, $\beta_3 = \alpha_2$, and $\beta_4 = -\alpha_1$.

Scaling filters for Daubechies also possess the property of having energy equal to 1, just as the scaling filters of Haar: $\alpha_1{}^2 + \alpha_2{}^2 + \alpha_3{}^2 + \alpha_4{}^2 = 1$ and the $\sqrt{2}$ shows up again with $\alpha_1 + \alpha_2 + \alpha_3 + \alpha_4 = \sqrt{2}$. For the Daubechies wavelet filters, as with the Haar filters, $\beta_1{}^2 + \beta_2{}^2 + \beta_3{}^2 + \beta_4{}^2 = 1$, $\beta_1 + \beta_2 + \beta_3 + \beta_4 = 0$.
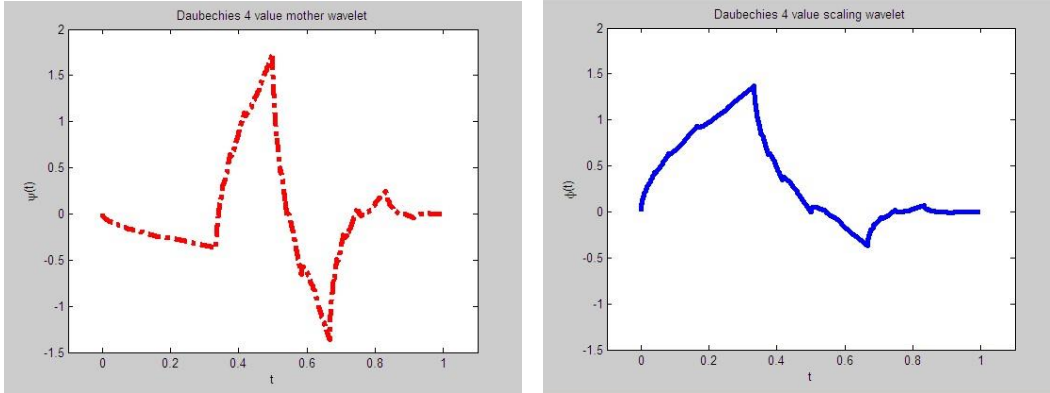
Figure: 2.15 The Daubechies wavelets
(a) The Daubechies mother wavelet ($\psi(t)$)   (b) The Daubechies scaling wavelet ($\varphi(t)$)

2 octaves of the signal have been shown in the fig 2.16 for the same signal that was shown in fig 2.8(a).

Figure 2.16 shows two octaves of the same original signal as we have seen figure 2.8(a). Successive inclusion of high pass and low pass more values have also been observed for the other type of Daubechies wavelets. The filter coefficients can offer longer support to the Daubechies wavelets. This support may be two times as that of Haar wavelet. By comparing the figures 2.16, 2.17 and 2.8, the comparison of Haar and Daubechies wavelets could be made.

Figure 2.16 Two octaves of the Daubechies transform of a signal
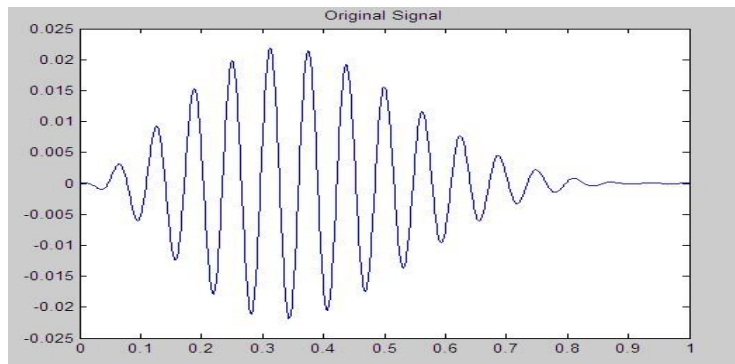
Figure 2.16(a) The signal $x^2(1-x)^4 \cos 32\pi x$
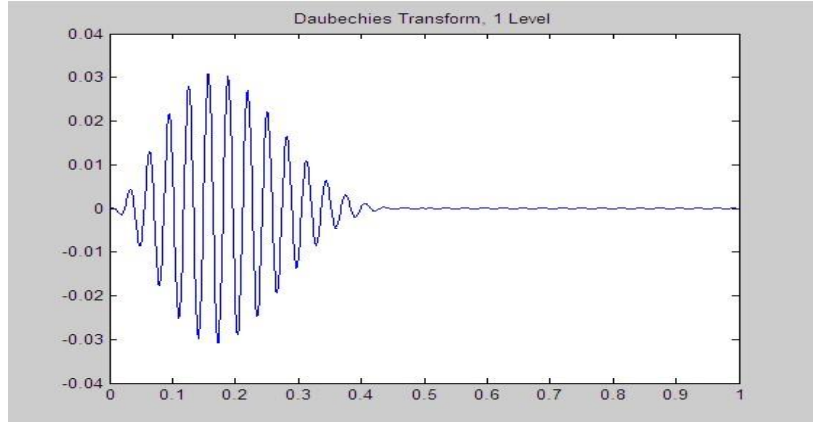
Figure 2.16(b) Daubechies Transform 1 Level
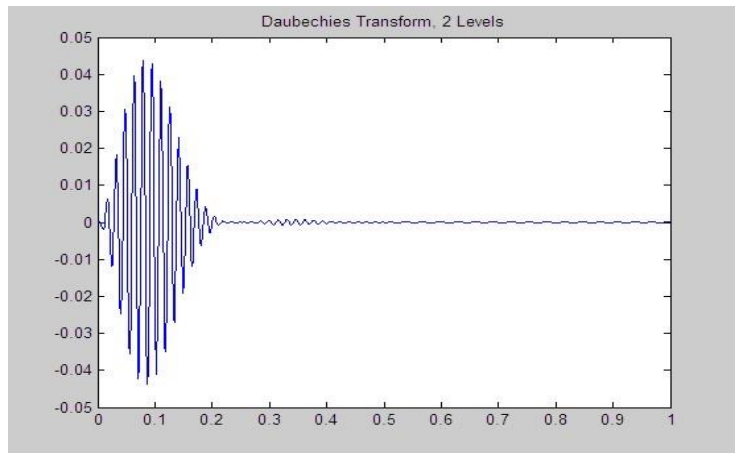
Figure: 2.16 (c) Daubechies Transform 2 Levels

Figure 2.17 Two octaves of the Daubechies 64 filter coefficient transform of a signal

Original Signal
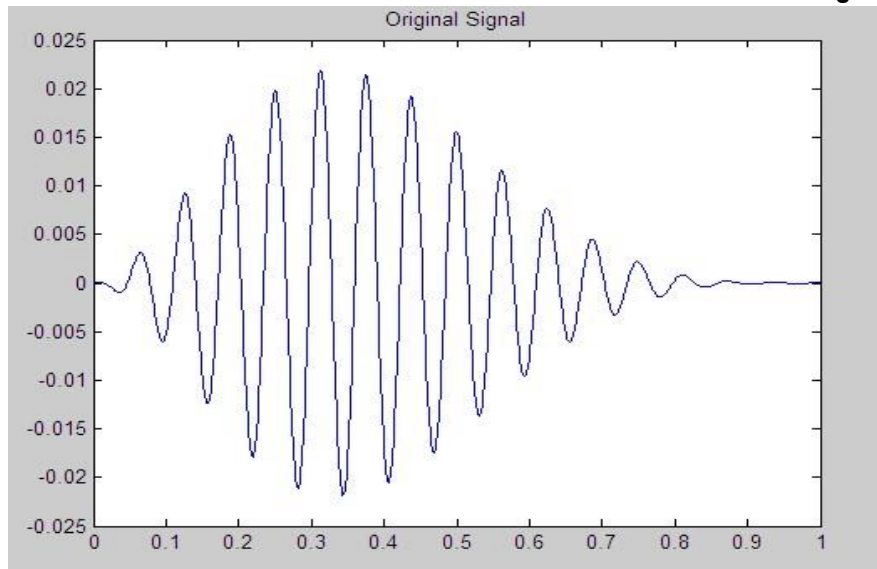
Figure: 2.17 (a) The signal $x^2(1-x)^4\cos32\pi x$

Daubechies 64 filter cofficient transform, 1 level
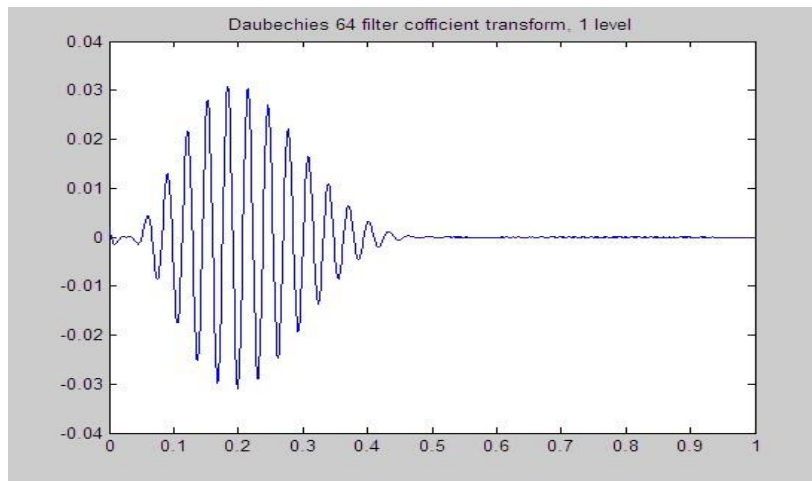
Figure: 2.17 (b) Daubechies 64 filter coefficient transform 1 Level
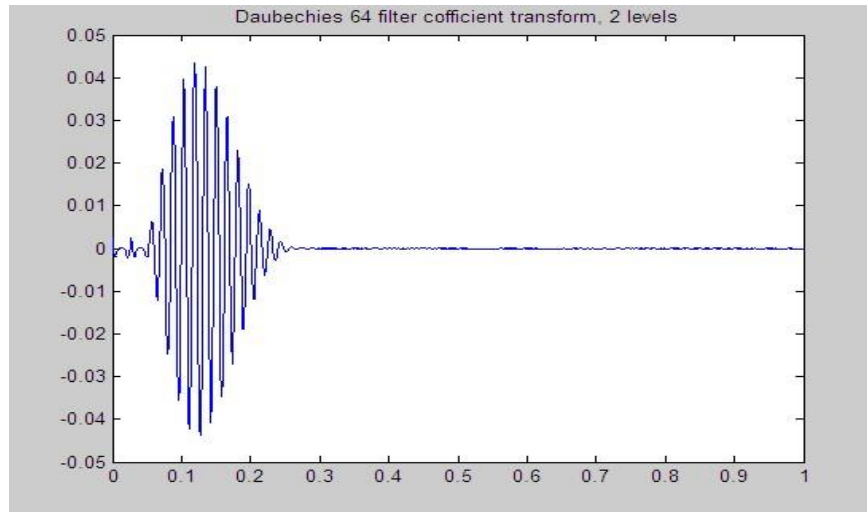
Figure: 2.17 (c) Daubechies 64 filter coefficient transform 2 Levels

Another wavelet family of interest is known as Coiflets which is created from family of Daubechies wavelets. It is named after its inventor Coifman who designed it for retaining the close matching between the original signal and its approximation.

A wavelets mother pair (ψ and ψ') along with the pair of scaling wavelets φ and φ') is utilized in Biorthogonal wavelets. The reconstruction and decomposition are allowed by each of these two. So, enabling the possibility of reconstruction for the resulting wavelets while eliminating the necessity of orthogonality.

CHAPTER 3

Estimation of vectors

3.1 Introduction

For video, de-noising detail wavelet coefficients have correlation among them as indicated by, following table 3.2. HH, HL and LH, are diagonal, horizontal and vertical sub bands of detail wavelet coefficients correspondingly. A technique which is called multivariate estimation, is applied on local neighborhood vector wavelet coefficients to build a de-noiser which is capable to exploit both types of correlations.

An existing model which is Gaussian Scale mixtures model assumes that each wavelet coefficient neighboring vector is jointly Gaussian. For each possible value of coefficients for scaling, neighboring vectors are used to compute conditional probabilities. Least square estimator for Bayesian could be obtained by weighing the scaling coefficients' conditional probabilities estimated by the integration of Linear MMSE.

We extended the concept of scaler HMT based de-noising to vector wavelet HMT [13,14]. It has close similarities to Scalar GSM based de-noising with binary coefficients of scaling. But a slight variance exists in the estimation of scaling coefficients' posterior probabilities. Approaches based of GSM type systems, makes independent estimation for every vector in wavelet whereas Hidden model tree approach estimates collectively over all coefficients of quad tree wavelet. Moreover, model based on GSM undertakes that correlation matrix for signal is supposed to remain same for different scaling coefficients with varying values. But HMT model gives the advantage of allowing covariance matrix modelled on the basis of state independence.

HMT based wavelet de-noising approach treats wavelet coefficients detail, as the pdfs are modeled by random variables models their probability density function as a Gaussian distributions combination with zero mean corresponds to Large and small states as L and S:

$$p(x) = p(S)N\left(0, \sigma_{x|S}^2\right) + p(L)N(0, \sigma_{x|L}^2)$$

p(L) and p(S) are prior state probabilities, whereas variance in the two states are represented by $\sigma_{x|S}^2$ and $\sigma_{x|L}^2$.

If x is the coefficient of wavelet and the noisy version $\tilde{x}$ is:

$$\tilde{x} = x + n$$

The noise component is supposed to be Gaussian with a mean of zero which has σ_n^2 variance, and $\tilde{x}$ is conditioned Gaussian with zero mean and $\sigma_{x|q}^2 + \sigma_n^2$. mean estimate for the two terms is linear when conditioned as follow:

$$E(x|\tilde{x}, q) = \frac{\sigma_{x|q}}{\sigma_{x|q}^2 + \sigma_n^2} \tilde{x} \qquad (3.1)$$

Signal and noise are supposed to have no correlation between them. Through chain rule of when $\tilde{x}$ is provided, for x the conditional mean could be acquired as follow

$$\tilde{x} = E(x| \tilde{x}) = \sum p(q| \tilde{x}) \frac{\sigma_{x|q}^2}{\sigma_{x|q}^2 + \sigma_n^2} \qquad (3.2)$$

By making assumptions about the independent states, p (q| $\tilde{x}$) could be predicted. Yet, with the addition of correlations at inter scale level into the prediction can provide good results in terms of de-noising. For the determination of conditioned state probabilities standard algorithm working in the upward-downward manner could be utilized.

3.1.1 Upward-Downward algorithm

Upward-downward algorithm is used to estimate hidden state variable probabilities.

In upward step, propagation is carried out in upward way along the tree while in downward step, propagation is down the tree.

Three parameters' groups are required by this algorithm.

1- The preceding probabilities of state p(C) and p(S)
2- Conditional variances $\sigma_{x|S}^2$ and $\sigma_{x|L}^2$
3- State transition matrix parent child $p(q_i|q_j)$

Crouse et al. proposed an algorithm for the estimation of these groups of parameters for each scale which is called Expectation maximization (EM) algorithm.

For exploiting any possible correlation existing in the sequences of vide the Scalar estimation can be subjected to extension. The neighboring elements may be same scale coefficients or can have the similar positions in neighbor scales.

3.2 Maximization of Expectation algorithm

The algorithm of Expectation maximization is a general mechanism for approximately obtaining maximum a posteriori (MAP) or maximum likelihood for predicting the characteristics of distribution that underlies in the given set of data for making up for the missing values.

Hidden Markov Model HMM could be one such example where hidden variables are not observed and we can say that some data is missing. Another example is in a Mixture model where expectation maximization algorithm could be applied. A number of concealed variables are existing in these models and Expectation Maximization algorithm is a way to tackle such problem of missing information or concealed variables. EM has the special characteristic that it exploits the structure of particular types of problems. Usually the probability of all the data that is observed (even hidden data), it emerges from the exponential function's family and hence, the Expectation Maximization is therefore applicable.

Algorithm of expectation maximization has two fundamental areas of applications. The first one involves the scenario when there are missing values in the data because of the constraints imposed by the process of observations. The second area of application is encountered when the optimization of likelihood function becomes inflexible in terms of analysis. However, when assumptions could facilitate the estimation of likelihood function, the hidden parameters can be subjected to assumptions. In the community of pattern recognition computations, the additional hidden values estimation may find its applications.

3.2.1 Introduction

In statistical Signal Processing, EM algorithm is an iterative scheme to discover the maximum likelihood. It could also be referred to as maximization of MAP estimation within the

models of statistics, meanwhile the reliance of models lie in the variables that cannot be observed and are latent. The iterations of expectation maximization algorithm keep on alternating between the step of expectations E and the step of maximization M. The expectation step formulates the functions for the likelihood by exploiting the predictions made for the varying parameters whereas the step of maximization of the estimated log likelihood in the first step. The estimation of parameters is further utilized for the distribution determination associated with the latent variables in E step.

For finding maximum likelihood or maximum a posteriori (MAP) estimates of parameters in statistical models, where the model depends on unobserved latent variables. The EM iteration alternates between performing an expectation (E) step, which creates a function for the expectation of the log-likelihood evaluated using the current estimate for the parameters, and maximization (M) step, which computes parameters maximizing the expected log-likelihood found on the Estep. These parameter estimates are then used to determine the distribution of the latent variables in the next E step.

3.2.2 Mathematical Investigation

Applicability of Expectation maximization algorithms exist for such models that are having some data missing or latent variables such as Hidden Markov Model. There is some observable data available for the model which is represented as $Xn = (x_1, \ldots, x_i)$. Xn is the data that is desired for modeling.

Model exists in terms of random variables X and Z that have a certain joint distribution P_θ for some unknown parameters $\theta \in \Theta$. This P_θ belongs typically to the exponential family and that's where Expectation Maximization algorithm really becomes prominent. Maximization of the marginal probabilities such as that of X_i is the intended goal of this work. Due to the Z being latent variables, maximization of probabilities cannot be accomplished:

$$\theta_{MLE} \in argmax_\theta \ P_\theta \ (x) \tag{3.3}$$

Problem is encountered in the maximization of probabilities that is also presented in the equation 3.4. Due to the summation over RV Z, it produces multimodal data which shows the possibility of maxima being more than a single one. Moreover, when the mathematical examination if equation is carried out such as taking derivative, it ends up to an analytical

expression that is nearly impossible to get a solution for. These issues can be resolved by using the EM algorithm.

$$P_\theta\ (x) = \ \Sigma_Z\, P_\theta\ (x, z) \qquad\qquad (3.4)$$

EM algorithm addresses this issue by iteratively improving the estimate of parameterθ. It iteratively computes the E and M steps shown as follows. Alternating between the E and M steps till convergence leads to a unique maximum.

E-Step: $\qquad\qquad\qquad\qquad Q^{(\theta,\ \theta_t)} = \ E_{\theta_t}\ (\log P_\theta\ (X, Z)|\ X = x) \qquad\qquad (3.5)$

M-Step: $\qquad\qquad\qquad\qquad \theta_{t+1}\ \in\ argmax_\theta\ Q\ (\theta,\ \theta_t) \qquad\qquad (3.6)$

3.3 HMT of Wavelet Coefficients

As discussed earlier, HMT models are used to capture the mutual wavelet coefficient dependences through modeling of statistical properties of wavelet coefficients. Markovian dependencies tie together the hidden states assigned to the coefficients rather than their values, which are thus treated as independent of all variables given the hidden state. Owing to the secondary properties of wavelet, HMT deals with coefficients as;

- For matching the opposite nature of wavelet coefficients to the Gaussian distribution, each coefficient's marginal probability density function is modelled by the Hidden Markov tree as GM density with states that are hidden regardless of the size of coefficients.

- For capturing the level of dependence among various coefficients of wavelet, Hidden Markov tree utilizes a tree of probabilities.

The important features of the distribution of wavelet coefficients like persistence and clustering is also considerable for the modelling of statistics addition to marginal statistics of DWT that are captured by IMM. Hence, a Hidden Markov tree model was developed for the wavelet domain in which the nodes are connecting on vertical scales with the Markov chains (fig 4-6). Hidden Markov tree is a GMM with multiple dimensions that implements the Markov chains with structures of tree form over the scales for capturing the dependency that exists between various wavelet coefficient scales.

The Hidden Markov tree has been applied in the processing of images whereas HMT has a framework of quad-tree that is described in 3 DWT sub-bands individually.

Figure 3.1: HMT

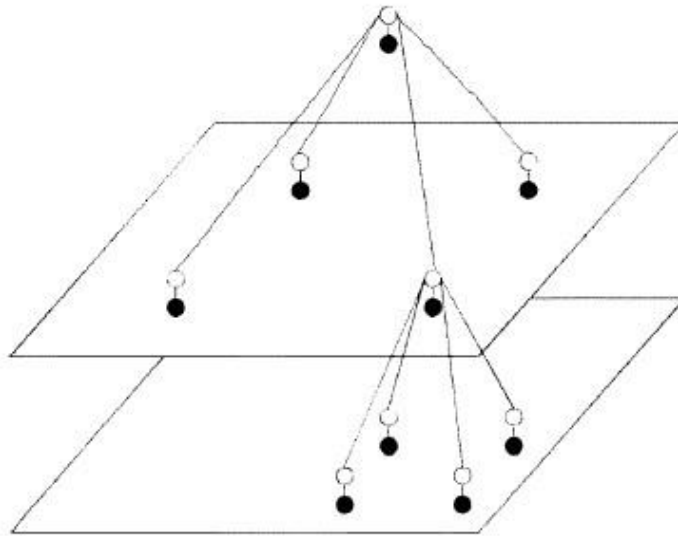The neighborhood in the proposed model gets restricted to 3 color constituents (RGB) its gray scaled version with neighboring frames as 2K, which leaves us with $M = 6k + 3$

IF the corrupted version of x is $\tilde{x} = x + n$, the zero-mean noise with Gaussian distribution is the reason behind corruption. If the state of x_i is s_i , s is vector including every state of coefficients in x.
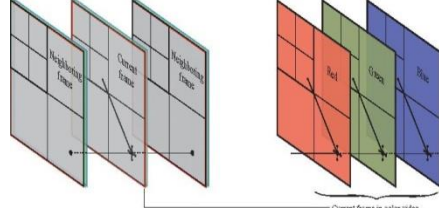
Fig 3.2 Vector coefficient K1 in video sequence

As signal vector and its noisy form are provisionally Gaussian, given the x̃ and s being its linear function, the minimum mean squared error (MMSE) estimation of x is provided as .

$$E(x|\tilde{x}, s) = \sum x|s \left(\sum x|s + \sum n\right)^{-1} \tilde{x} \quad (3.7)$$

Where$\sum_{n \text{ and }}$ $\sum_{x|s}$ are the noise covariance and conditional signal matrices respectively.

Mean estimate of x conditioned by a given $\tilde{x}$ is

$$E(x|\tilde{x}) = \sum p(s|\tilde{x}) \sum x|s \left(\sum x|s + \sum n\right)^{-1} \tilde{x} \quad (3.8)$$

Where $p(s|\tilde{x})$ is conditional probability of state s given x̃. Since the number of summation increases exponentially with the vector size K, estimation is difficult to compute.

We assume all coefficients in same state which is q, to avoid complexity and we are using following estimator

$$\sum p(q|\tilde{x}) \sum x|q \left(\sum x|q + \sum n\right)^{-1} \tilde{x} \quad (3.9)$$

GSM based approach [15] has similar assumption, where components have same scaling coefficients.

3.4 VECTOR HIDDEN MARKOV TREE

Scalar Hidden Markov tree uses downward upward algorithm [3] for estimating conditional probability of p(q|x).in scalar HMT, the prior state probabilities p(q), parent-child conditional variances q, and state transition matrix p(qi|qj) are worked in algorithm named as upward-downward.

Conditional pdfs of scalar are defined by conditional variances as

$$p(x|q) = \frac{1}{\sqrt{2\pi\sigma_{x|q}^2}} ExP(-\frac{x^2}{2\sigma_{x|q}^2}) \qquad (3.10)$$

Table 3.1 Two states average inter-frame correlations

	S		L	
Scale	k&k+1	k&k+2	k&k+1	k&k+2
1	0294	0.058	0.546	0.039
2	0.628	0.338	0.753	0.334
3	0.851	0.677	0.924	0.751
4	0.952	0.879	0.976	0.921
5	0.983	0.949	0.993	0.977

Unknown parameters are estimated by using algorithm of EM [3] and through collection of predefined general factors [4].

Algorithm of Upward-downward approach is stretched to vector x by putting $\sigma_{x|q}^2$ for $\sum_{x|q}$. Vector conditional probability density function is given as

$$p(x|q) = \frac{1}{\sqrt{(2\pi)^M \det\Sigma_{x|q}}} exp(-\frac{x^T \Sigma_{x|q} x}{2}) \qquad (3.11)$$

One of the most straightforward way of estimating unknown parameters is to extend algorithm of EM [3] to higher dimension. For avoiding iterations scalar model is extended to vector. The disadvantage of this approach the modelling of characteristic variability of correlations existing between frames. The example of video "FOREMAN" in which the horizontal motion results in greater correlation between the frames in the LH sub-bands that is different from the HH and HL sub-bands, which is presented in table 3.2. The vertical motions in the video results in greater correlations between the frames in sub-band HL.

Table 3.2 wavelet coefficients of video "FOREMAN"

Scale	Frame k & k+l			Frame k & k+2		
	LH	HL	HH	LH	HL	HH
1	0.781	0.462	0.387	0.437	-0.147	-0.168
2	0.904	0.708	0.645	0.710	0.197	0.097
3	0.972	0.913	0.882	0.912	0.711	0.628
4	0.992	0.974	0.962	0.974	0.909	0.879
5	0.998	0.993	0.989	0.993	0.974	0.963

We have proposed the utilization of correlation matrix for computation of conditioned state probability. We have updated conditional signal covariance matrices by using following equation

$$\Sigma_{x|q} = \frac{\sum_{x \smallsmile} x x^T p(q|x)}{\sum_x p(q|x)} - \Sigma_n$$

C h a p t e r 4

4.1 Spatio-Temporal filtering

Motion blur or additive noise often results in the corruption of video signals. So, it is desired that the de-noising of signal is performed for removing the impact of noise that has corrupted the signal. It is very common that the noise is modelled as a random process with Gaussian distribution which has no dependence on the original signal. For the adequate de-noising of signals under such circumstances, techniques of statistical signal processing are utilized. For processing the noise corrupted signals of video, we have implemented the filtering process by Wiener filters. These are the most appropriate filters for the task as they can provide the minimization of mean square error between the recovered and original signal. The video signal has also been modeled as HMM and Kalman filter has been implemented for proceeding with the removal of noise. Lastly, by comparing these methods with the traditional techniques of nonlinear filtering such as soft coring and median filtering. The following is the basic outline of this dissertation:
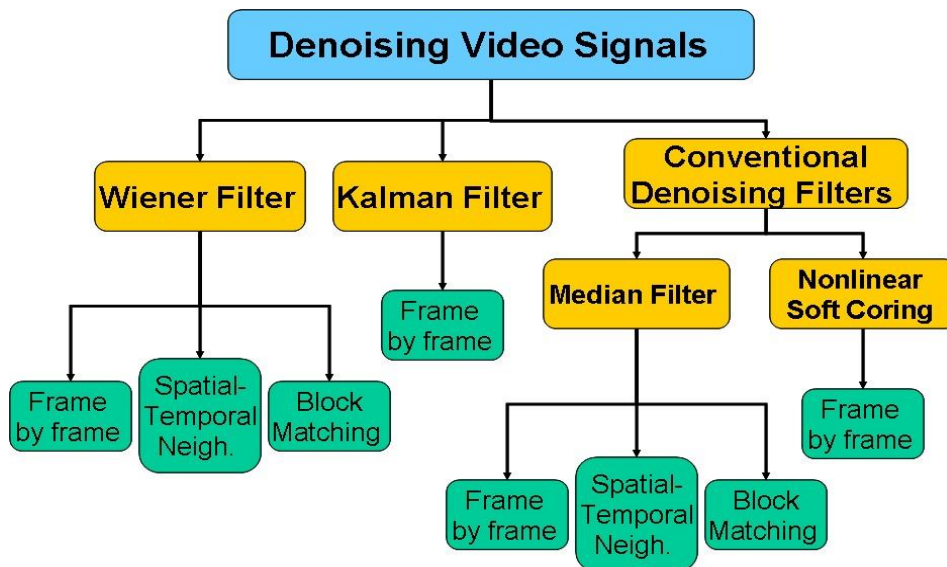

Fig 4.1: General outline

4.1.1 Wiener Filter

The restoring mechanism for De-convolving such as by acquiring knowledge of image being blur for certain type of filter, the process of inverse filtering can recover the images. Regardless of the restoring properties, inverse filter is likely to affect by additive noise. The method of single degradation per instant, provides the ability of developing algorithm of restoration for every degradation and merge them in simple manner. An optimal tradeoff is executed by the Wiener filtering between smoothing of noise and inverse filtering. The additive noise is removed by it and whereas the blurring is inverted in parallel of noise removal.

The mean square error characteristics of Wiener filtering makes it an optimal choice for filtering. Simply speaking it keeps mean square error minimized in the process of de-noising and inverse filtering. It offers the original signal's linear estimate. The modeling finds its roots in the stochastic background. The principal of orthogonality gives the Fourier domain illustration of Wiener filter:

$$W(f_1, f_2) = \frac{H^*(f_1, f_2)S_{xx}(f_1, f_2)}{|H(f_1, f_2)|^2 S_{xx}(f_1, f_2) + S_{\eta\eta}(f_1, f_2)},$$

The blurring filter is represented by $H(f_1, f_2)$ and $S_{xx}(f_1, f_2), S_{\eta\eta}(f_1, f_2)$ are respectively power spectra and additive noise of the original signal. It is evident from the analysis that two parts of Wiener filter are there one of which aims at smoothing of noise (LP) and the other one is focused on the inverse filtering (HP).

4.1.2 Implementation:

For practically carrying out the implementation of Wiener Filter, the original video frame's power spectra along with the addition of noise has to be estimated first. For the additive noise to be white noise variance of noise is supposed to be equivalent to the power spectrum. There are a number of methods available for the power spectrum estimation of the video signal. A

periodogram is the method of conduction direct estimate from observations as:

$$S_{yy}^{per} = \frac{1}{N^2}[Y(k,l)Y(k,l)^*]$$

Y(k,l) is the observation's Discrete Fourier transform. Such an estimation has the benefits of easy implementation without concerning about the inverse filter being singular. Following is an expression of another cascades implementation of the similar kind:

$$S_{xx} = \frac{S_{yy} - S_{\eta\eta}}{|H|^2},$$

That is simply resulted from the fact $S_{yy} = S_{\eta\eta} + S_{xx}|H|^2.$ By making use of the periodogram estimator, power spectrum which is denoted as S_{yy} can be estimated. This results in the estimation of noise smoothing and inverse filtering cascade implementation:

$$W = \frac{1}{H}\frac{S_{yy}^{per} - S_{\eta\eta}}{S_{yy}^{per}}.$$

The drawback of such an implementation lies in the singularity of inverse filtering as the use of inverse filtering is generalized. It is also suggested often that estimation of original image's power spectrum can be based on a model as $1/f^{\alpha}$.

4.1.3 Results from experimentation

For presenting the Wiener filter in restoration of frame 256x256 standard of salesman video frame is being utilized. Low pass filter is used for blurring the frame.

$$H = \frac{1}{16}\begin{bmatrix} 1 & 1 & 1 & 1 \\ 1 & 1 & 1 & 1 \\ 1 & 1 & 1 & 1 \\ 1 & 1 & 1 & 1 \end{bmatrix},$$

Then put the variance of AWGN as 100 in the blurred frame. The application of Wiener filter is followed by the inverse filtering and noise smoothing in cascaded implementation. Frames have been enlisted along with the PSNRs as follow. The visual performance of frames being restored has shown improvements in the process.

| Standard Salesman video frame PSNR = Infinity | Blurred Salesman frame PSNR = 23.2993 | Restored Salesman frame PSNR = 19.1447 |

Fig 4.2: Test Salesman frame and Blurred frame

4.2 Kalman Filter

Considering *X(n)* and *Y(n)* as random processes:

$$X_{n+1} = A_n X_n + W_n \qquad (4) \qquad\qquad Y_n = H_n X_n + N_n \qquad (5)$$

N_n and W_n are independent random processes with Gaussian distributions.

Equation 4 is an obvious representation of a Markov process whereas the equation 5 shows an HMM process.

The probability of X_n being conditioned by Y^n, $p(X_n | Y^n)$ is needed for estimating the value of random variable X from the observations made on Y. Recursion algorithm of forward nature is needed for accomplishment of such estimation goals.

For the sake of application to the video signals the two previous equations such as (6) and (7) have been subjected to particular definition of parameters. W_n represents random process of Gaussian distribution, X_n shows the current and X_{n-1} shows the previous value of pixel. Noisy observation is represented by Yn in the equation. The assumption of Kalman Filter about the independent Gaussian process are held by this model:

$$X_n = X_{n-1} + W_n \qquad (6)$$

$$Y_n = X_n + N_n \qquad (7)$$

where σ_n^2 is the noise variance about whom assumption is made to be known and the process w has a variance of σ_w^2. The estimation of W's variance begins with the pixel values' mean estimation in the previous frames' μ_{n-1} matching blocks and frames that surrounds the present frame denoted as μ_n and in the previous frame. Estimation of σ_w^2 results in $\hat{\sigma}_w^2 = (\mu_n - \mu_{n-1})^2$.

As W attempts for capturing the variations existing between the successive frames' pixels, the estimate of σ_w^2 becomes a reasonable one. Furthermore, the initialization of β_0 to variance and mean as $\beta_0^{(0)}$ and $\beta_0^{(1)}$ is made for the initial frame.

Also, we initialize $\beta_0^{(0)}$ and $\beta_0^{(1)}$ to the mean and variance of X_0 which we estimate from the first frame. The most appropriate X_n estimate results as $E(X_n \mid Y^n)$ provided conditional probability of $p(X_n \mid Y^n)$. It should be noted that $E(X_n \mid Y^n)$ is $\alpha_n^{(0)}$. Section five presents the results of simulation.

During the recording process noise, has been added to the video. The problem is significant when the analog signal converted into a digital one. The undesirable feature not only lies in the affected quality of video but also in the degraded performance of overall system of processing.

A Kalman filter approach based on spatiotemporal setting has been approached in the previous literature to de-noise the video [1]. A three-dimensional AR model would be needed in such an approach. Results had been shown along with the parameters associated with the estimations conducted by this model from the original sequence of video that had no noise added to it. Furthermore, at every pixel, the state vector dimensionality has been observed to be very high. So, the amount of required storage and computations has been increased for processing of at individual frames.

45

Adaptive filter with linear MMSE was proposed in [2] for the compensation of temporal motions. A vigorous algorithm has been proposed by Fogel [3] that is used here in the estimation of motion. The approach of denoising that has been adopted is similar to that of Kaun [16] which aims at providing the adaptive filtering with linear MMSE. The algorithm for estimation of motion appears to have higher costs of computation, eight values, four vectors would require storage for every pixel along with the storage exhaustion by frames.

Filter with weighted averaging working in adapted fashion was proposed in [4]. The reliance of this approach is centered on the idea the pixels' averaging in spatiotemporal environment is likely to provide better estimation about the intensities of the pixels remaining nearly the same. When a certain pixel's intensity exceeds the chosen threshold, it is implicated that it is an outlier because it has been affected by the noise and doesn't contribute to the averaging. The rest of pixels have been averaged to see their deviations from the existing values of pixel. Such a scheme appears to be very appropriate for the lower SNRs and when the content is subjected to abrupt variations.

Similarly, in the work of [17] a wide-ranging evaluation of techniques for the de-noising of video signals has been presented.

The scheme proposed in our work spatial and temporal are performed separately first and then are integrated together. By utilizing the single dimensional Kalman filter, exploitation of temporal redundancy is performed. The intensity value of each pixel which is a scalar one, is provided by the states of Kalman filter at every pixel. By using the information of previous and current states, a novel method of estimating noise state variances in adaptive manner without having to restore the cleaner original frames is presented. Pixel block in integer is simply utilized here:
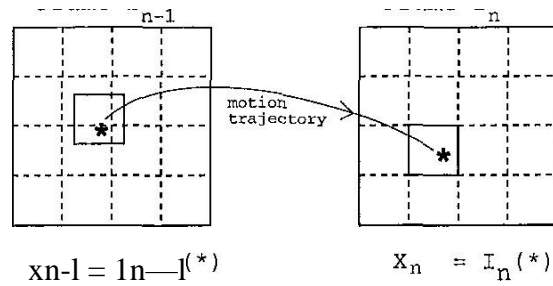
$$xn\text{-}l = 1n\text{---}l^{(*)} \qquad X_n \; = \; I_n(*)$$

Figure 4.3: System Model for establishing the Kalman Filtering Equations.

The spatial redundancy is exploited using the adaptive edge preserving Wiener filter proposed by Kuan [16]. Simple averaging has been utilized for combining the two estimations so that final frame in de-noised form could be obtained.

These two estimates are then combined using simple averaging to get the final denoised frame. Parting of temporal and spatial processing, simple block matching for scalar state and motion estimation Kalman filter brings fast computational abilities to the scheme. Moreover, only the 2 values per pixel and the previous frame are needed for storage that reduces the storage requirements of processing.

Signal to noise ratio performance of our scheme for the foreman, Trevor and Susie sequences is comparable to the results in [1, 2, 4] at much less computational and memory requirements.

4.2.1 Temporal Kalman Filtering

The system is presented by the fig 1. Discrete time instances at which the frame of videos is reaching, have been denoted by 'n'. If a pointed object' s motion has to be tracked as indicated by * in the fig.

The concentration of this object in the current (original) frame in is denoted by xn and in the earlier frame in—I is denoted by xn —1. Ideally xn = Xn—l but because of occurrence of error or because of variations in radiance we have xn - xn-l + Un (1)

where Un denotes the error, or advance in xn compared to xn -1, We shall call Un as noise of motion and it is modeled as Gaussian and independent from one-pixel location to another and also liberated in time. The computation of statistics and motion trajectory of Un are going to be discovered sooner in this research.

47

Original information about the intensity is usually affected and corrupted by the noise present during the video processing and hence our observation of the intensity xn is given by

$$Y_n = X_n + V_n \quad (2)$$

Where Vn denotes the noise that is undesired and intended to be removed. Modeling of VD also involves the Gaussian RV with zero mean and is independent of Un and AWGN in time and space. It could be noted that we can set (1) and (2) at all locations of pixels one by one in the present.

Due to various reasons, such as variations in illuminations, errors occurring in the estimation of motion and so on, the emergence of motion noise may take place. The intensity changes have been seen in the first equation as represented by the motion noise. In the absence of access to the original frames, we can estimate the variance of Un for alleviating the recording noise affects as (pn — where = mean (Bn) is the maximum likelihood estimate of xn assuming all xn are same in block Bn.

After which under certain conditions (Pn — ^{2} is most appropriate estimate of var (Un). Once the system of ours has been defined completely, the equations of Kalman filter are applied to make estimation of xn. By making use of the earlier frame's de-noised version, further improvements could be made. The motion vector for present frame can be calculated from the earlier one's de-noised version.

4.3 Nonlinear Filtering Techniques

4.3.1 Median Filtering

A nonlinear technique of filtering in which all pixels get replaced by the pixel values median.

Similarly, the neighborhood choice in the Winer Filter's application also becomes significant for the signal processing to be successful. The experiment has been conducted on varying types of neighbors to show the results being compared.

4.3.2 Soft Coring

Application of filtering techniques of non-linear nature to one frame is referred by the Soft coring in [17]. It is exploited in this technique that AWGN is basically possessing higher frequency with comparatively low amplitudes. The following figure represents the typical block diagram of soft coring. Furthermore, the typical curve α is also shown.
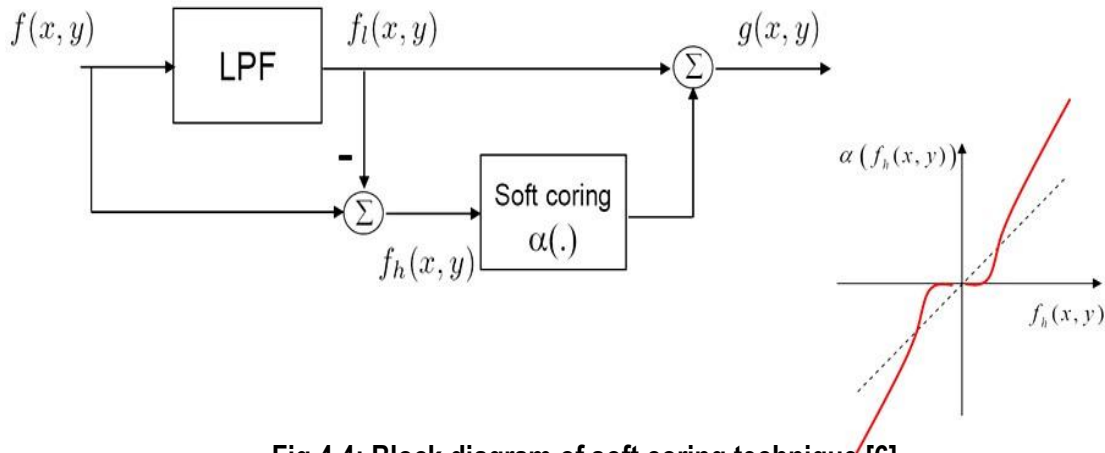

Fig 4.4: Block diagram of soft coring technique [6]

The signal $f(x, y)$ is made to pass through LP filter in the beginning for obtaining $f_l(x, y)$. Then this acquired signal is subtracted from the original one so that HP signal is also acquired. The higher value of HP signal of $f_h(x, y)$ would demand the preservation of an edge whose existence is conformed. Meanwhile, if the low values appear for high pass signal, noise could be expected in the flat background that will now be desired to be eliminated. These two filtered signals can eventually be used for the reconstruction of original signal again.

A routine of soft coring has so far been implemented on each frame on individual basis. However, it is safe to say that the designing of α () which a nonlinear function has been made in heuristic manner. The factors in this design of ours have shown good working for some of noise additions and did not perform well for the other values.

4.3.3 Results and Discussion

Fig 4.5: Wiener filter Mean Square Error with noise variance Fig 4.6 Results for different window sizes
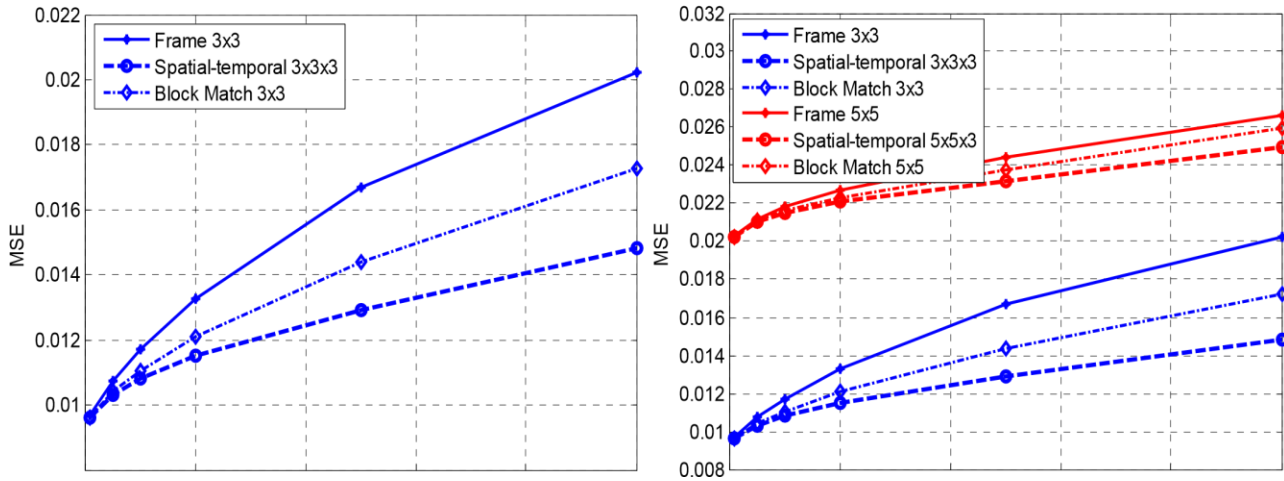
All of the proposed algorithms were tested on the selected standard video of "Foreman". The pixel values that have been normalized lies between 1 and 0 with the addition of variances and 0.1 and 0,001. At first, we have implemented the Wiener Filtering as demonstrated in the third section with 3 varying neighbors. At first the window size has been chosen to be 3 by 3. The mean square error values have been presented in the other figure as noise variance function. In the figure number 5, the changes that take place between the window sizing's to 5x5 from 3x3 are accounted for.

It is evident from the figures that by using the neighborhood of spatial-temporal for filtering, better results could be obtained as compared to the neighborhood with block matching. The use of information from three instead of two frames makes it possible. Furthermore, as there is only content with slow motion in the video, matching did not bring improvements in the performance in substantial way. It is believed by us that block matching must be doing better in the presence of high motions in the video content as neighborhood in spatial-temporal orientation are likely to have less accuracy when compared with the block matching.

It can be ducted from the fig 5 that results have been worsened with the increased window size which probably is due to the fact that filter is fundamentally a low pass filter. With the increased size of window, the Low pass effect has also increased and hence the blur effect on the image has enhanced with it.

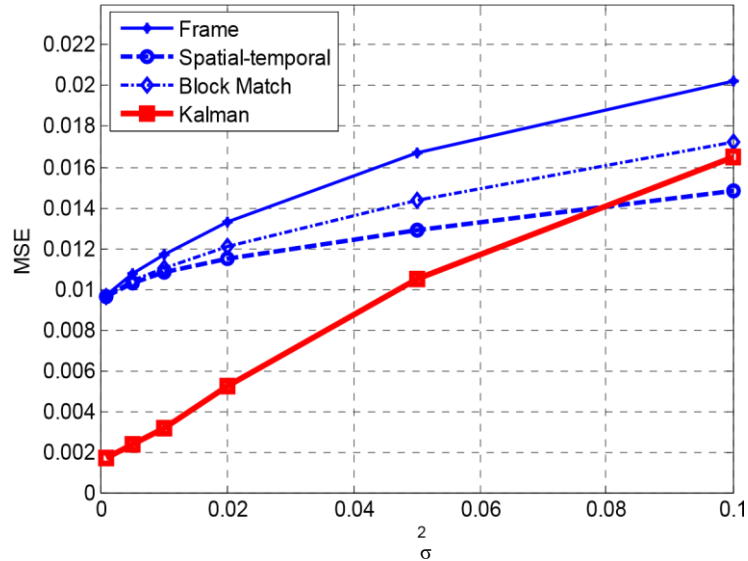The Kalman filter results are plotted in the Fig 4.7. Comparison with Wiener is also made:

Fig 4.7: Comparing Kalman and Wiener filters

It could be seen here that Kalman would perform bad in the low noise settings when compare with the Wiener filtering. But when the variances of noise are large, the two of them appears to have resemblance in their performances. Despite having a good noise removing job, the Kalman filter has shown sensitivity towards block matching, which is why the resulting video illustrated some blocking artifacts. By introduction of blocks of smaller size or interpolating the points, such problems could be eliminated.

Furthermore, we also have utilized the nonlinear techniques of conventional filtering in our work such as soft coring and the median filtering. The results of mean square error have been shown in the fig.7 along with the Wiener filter results.
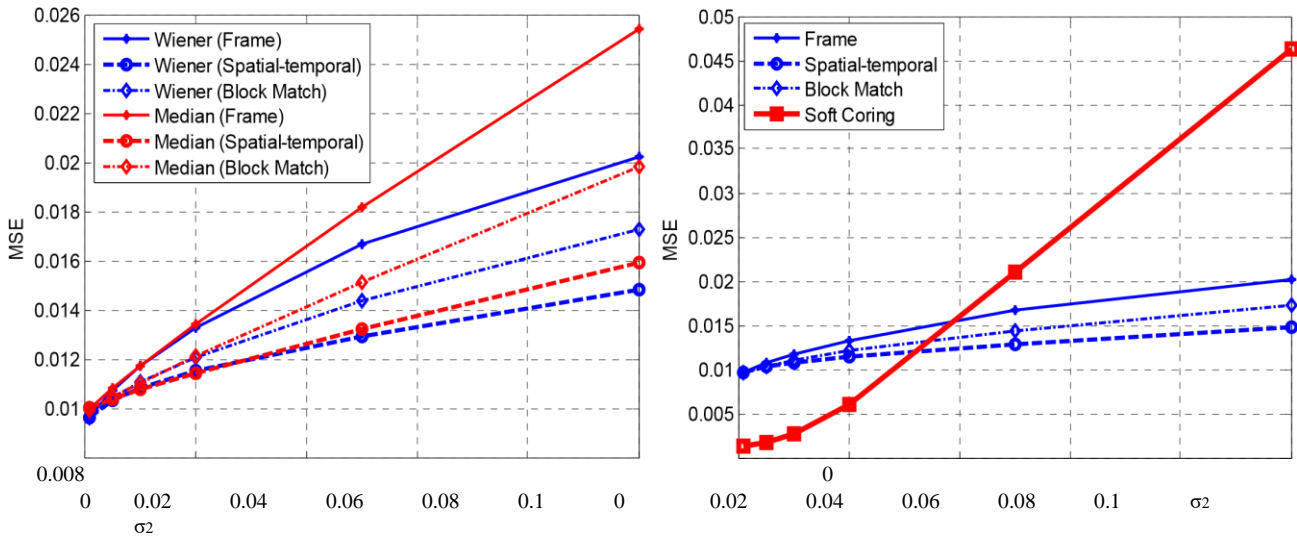
51

Fig 4.8: Conventional nonlinear filtering techniques

We have observed that for the regime of low noise, performance of soft coring is much better which becomes deteriorating with the increased variances in noise. As mentioned earlier, such characteristics have an association with the non-linear functions' parameters that have been selected and utilized in this experiment. It has been observed that performance of Wiener filtering at most of the levels has been better as compared to the median filter, However, it can also be said that the outperforming Wiener was not that significant and its results could be compared with those of median filtering. Such observations are very important as despite the linear estimation utilization, the performance has still managed to remain better than the traditional non-linear filtering mechanism.

At last we have compared the best possible accomplished results with all of the filtering techniques such as soft coring, Method 2 median filtering, Method 2 Kalman filtering and Wiener filtering.

52

C h a p t e r 5

Experiments and Results

Motivation behind progress of VEWC is fundamental WT's properties and, theoretical as well as pragmatic evidence supported by the different characteristics of technique have been explored. Though real testing of our technique is determined by image de-noising applications of it.

We compared the performance of our technique for video frame de-noising to other wavelet de-noising methods and filtering techniques. We have shown that our new structure offers important improvement in various well-studied standard problems.

VEWC is also appropriate in signal detection and classifications.

For performance evaluation of the proposed de-noising technique, experiments were conducted on the set of videos as shown in following tables 5.1-5.3, evaluation metric was CPSNR, a parameter that performs MSE measurements of the de-noised frames and is shown by following equation

$$\text{CPSNR} = -10\log_{10}\left(1/3\sum_{c \in \{R,G,B\}}\text{MSEc}\right)$$

5.1. Role of signal covariance matrix estimation

By using the limits in [18], the matrix for correlation computation is constrained between two states that may not be satisfactorily precise for de-noising dedications. We gave a new method, by updating the matrix using [19], before applying MMSE vector estimator [5]. As shown in following tables, such upgrading can bring improvements in the performance of CPSNR by 0.3 to 0.8 decibels. After few iterations improvement in performance will be less than 0.08db with eighty percent more cost on computation.

5.2 Comparison with older techniques

Table 5.1-5.3 compare the de-noising CPSNR performance between Wiener 3 filtering, CWDT, Kalman filtering, Median filtering and proposed vector estimation of wavelet

coefficients. As shown in tables Proposed technique improves CPSNR by 3-5 dB as compared to older techniques. Following figure is showing consistent behavior in all video frames.
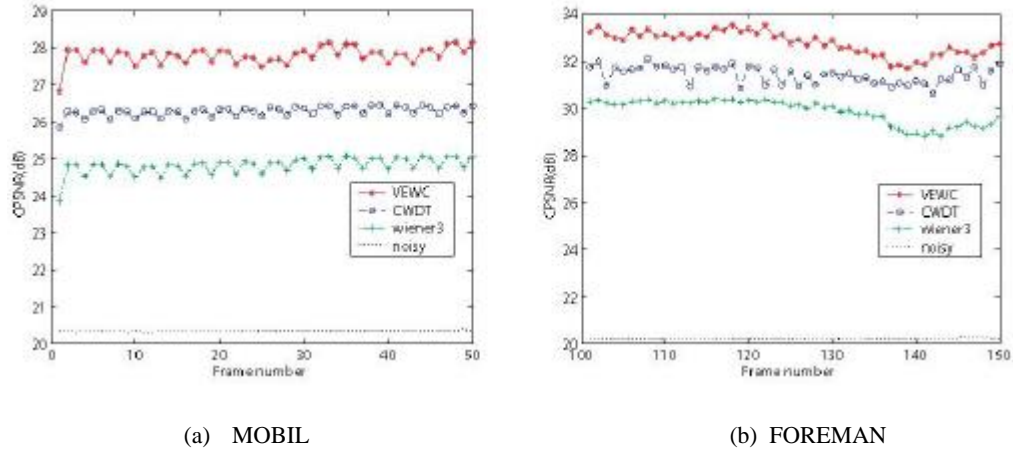

(a) MOBIL   (b) FOREMAN

Figure: 5-1 Comparison of CPSNR performance in video frames

Another technique which is Kokaram's approach, we compared our result with that, but performance of VEWC gives a gain of more than 7 dB while other one gave gain of 4 db.

We applied VEWC approach and other approaches to one frame of "GARDEN", VEWC de-noising preserved flower field edges better than other ones.

(a) Original   (b) noisy

(c) wiener 3

(d) CWDT

(e) VEWC

Figure: 5-2 Comparison of CPSNR performance in de-noised video frame of "Garden"

5.3 Proposed algorithm:

Proposed algorithm consists of following steps

1- Vector construction by joining the coefficients of wavelet at present T frame with the 2K neighboring frames.

2- Estimation of the signal correlation matrix [18] is applied to each sub band and universal model for "$\sigma^2_{x|q}$" for the computation of signal covariance matrix "$\sum_{x|q}$" as per [20]

3- Utilize "$\sum_{x|q}$" in algorithm named as upward-downward for the estimation of state probabilities that are conditional "$(P_{x|q})$"

4- On the basis of updated "$(P_{x|q})$", covariance matrices "$\sum_{x|q}$" should be updated as in [19]

55

5- Then apply that estimated parameter to MMSE estimator [5] in vector form, for de-noising wavelet coefficient of frame "F".

5.3.1 Simulation results:

We have applied VEWC to extracted video frames for standard videos like foreman, salesman and tennis (256 x256) with adjustable different variances. Three different variances are used in different approaches. Following experimental setting are being used Wiener filtering is used we have used CDWT Kalman filtering Median filter in the end our proposed VEWC technique. The PSNR of all images is compared with different de-noising algorithms. Comparison is done on the basis of different variances of Gaussian noise. Tables are showing their results.

Table 5-1: PSNR (dB) results for images corrupted with $\sigma = 0.05$

Frame (256x256)	Techniques for De-noising				
	Weiner3	CDWT	Kalman	Median Filter	**VEWC**
Foreman	26.2	23.0	26.3	26.7	**32.62**
Salesman	26.1	22.7	26.3	26.4	**30.4**
Tennis	21.3	21.8	25.3	25.0	**29.4**

Table 5-2: PSNR (dB) results for images corrupted with $\sigma = 0.1$

Frame (256x256)	Techniques for De-noising				
	Weiner3	CDWT	Kalman	Median Filter	VEWC
Foreman	20.9	20.7	23.5	23.7	**28.4**
Salesman	20.8	20.4	22.2	22.3	**26.9**
Tennis	21.3	21.8	22.3	22.1	**26.5**

Table 5-3: PSNR (dB) results for images corrupted with $\sigma = 0.2$

Frame (256x256)	Techniques for De-noising				
	Weiner3	CDWT	Kalman	Median filter	VEWC
Foreman	18.2	20.6	21.7	22.5	**22.02**
salesman	15.8	18.4	19.8	21.4	**23.3**
Tennis	18.6	20.8	21.8	22.6	**24.4**

As it is clear from the tables above, VEWC performs better in most cases as compared to other techniques.

## 5.3.2 Video frame De-noising:

To calculate and analyze our proposed algorithm, we compared our results with older techniques which are used for video de-noising. PSNR is the key factor which is the basis of comparison of de-noised video frames. Table 5-1, 5-2 and 5-3 are showing measured PSNR values for different σ_n. Different de-noising filters are used to characterized the results and comparison is carried out with the original results of the paper. The algorithm is applied on both standard video frames and other images of dimensions 256x256.Results are shown in following figures.
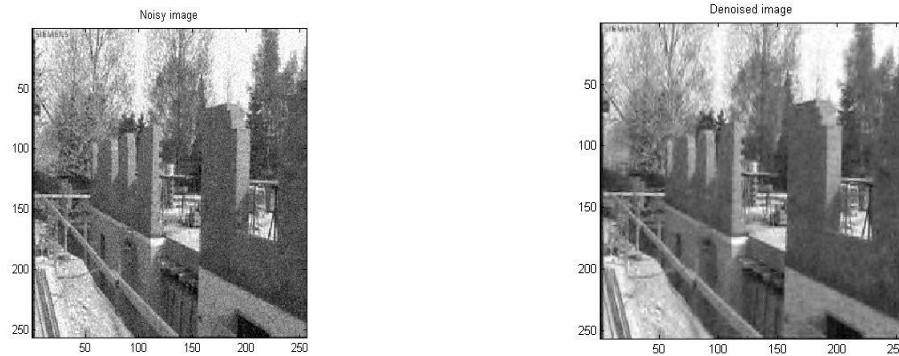
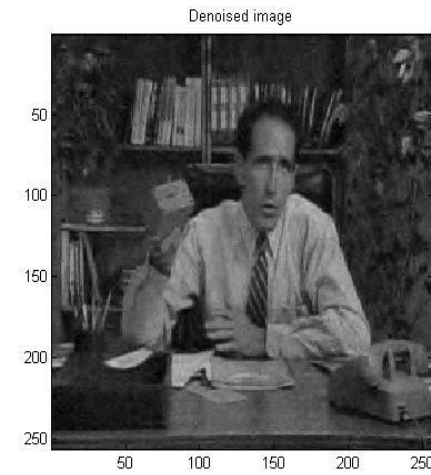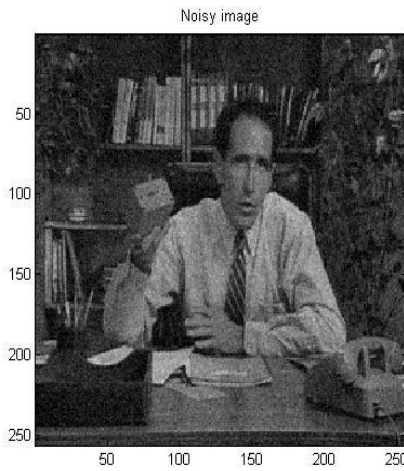PSNR of noisy image is 24.427dB   PSNR of de-noised image is 28.388dB

Figure 5-3: Noisy and De-noised image results for standard video frames with different σ_n
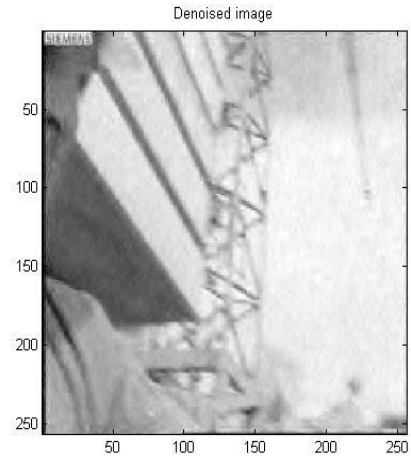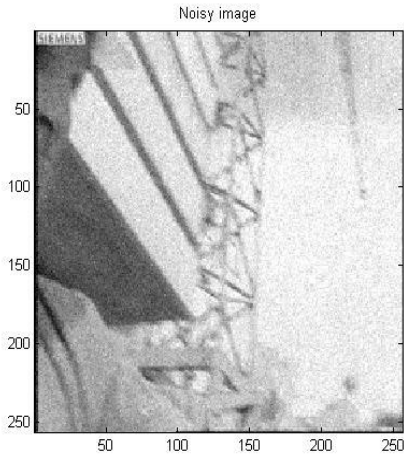
PSNR of noisy image is 14.018dB   PSNR of de-noised image is 22.0275dB
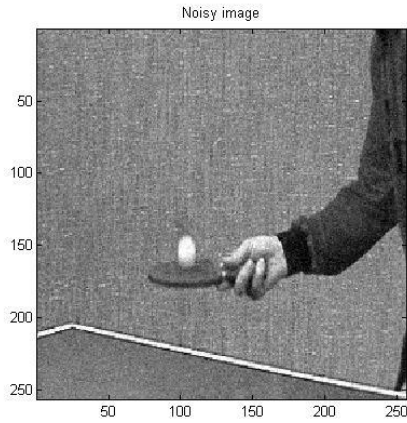
Figure 5-4: Noisy and De-noised image results for standard video frames with different σ_n
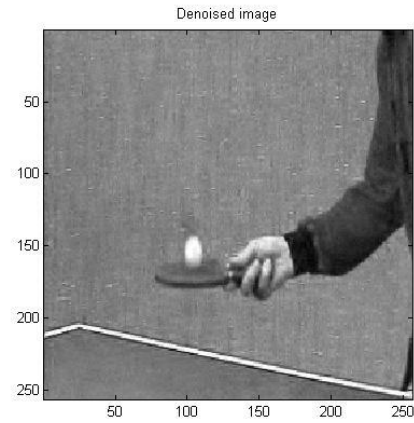

PSNR of noisy image is 26.0251dB   PSNR of de-noised image is 30.5965dB

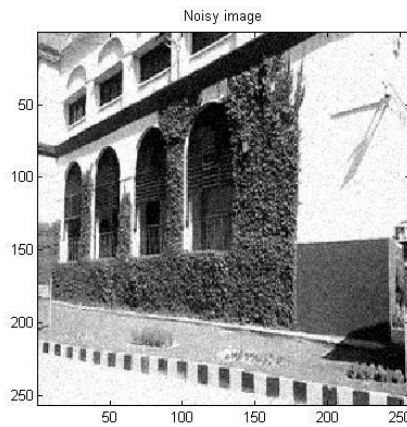**Figure 5-5: Noisy and De-noised image results for standard video frames with different σ_n**
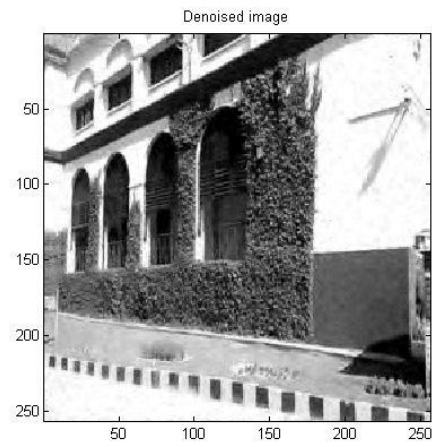
| PSNR of noisy image is 26.0281dB | PSNR of de-noised image is 29.6678dB |

Figure 5-6: Noisy and De-noised image results for standard video frames with different σ_n

We have also applied our algorithm on some local video frames of our institute. Results are shown in following three frames at different σ_n.
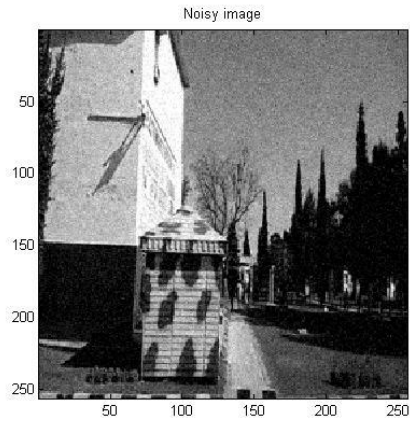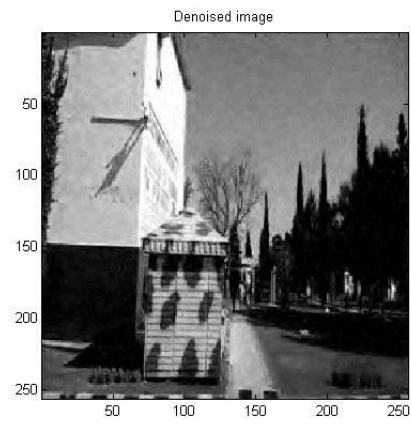

| PSNR of noisy image is 26.0302dB | PSNR of de-noised image is 28.2638dB |

Figure 5-7: Noisy and De-noised image results for local video frames with different σ_n
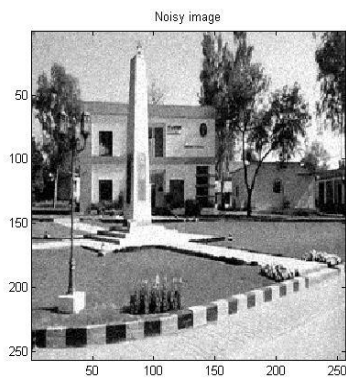
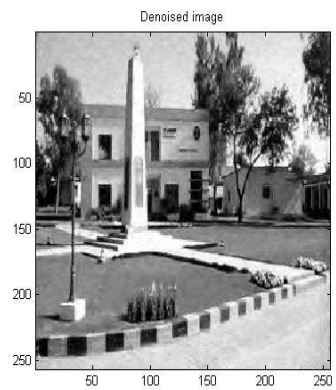PSNR of noisy image is 26.0059dB   PSNR of de-noised image is 30.1046dB

Figure 5-8: Noisy and De-noised image results for local video frames with σ_n = 0.05

PSNR of noisy image is 26.0455dB   PSNR of de-noised image is 28.9792dB

Figure 5-9: Noisy and De-noised image results for local video frames with σ_n = 0.05

C h a p t e r 6

6.1 Conclusion

In this thesis, video de-noising using Vector estimation of wavelet coefficients is debated. The initial portion of the thesis was dedicated to provide introduction to wavelets in general way. Vector estimation of Hidden Markov Tree model was also explored with their mathematical modeling so that essential understanding for the dissertation could be developed. The HMT model has been explored in detail alongside its significance in the signal processing.

The later part of the thesis, included various techniques for video de-noising are discussed and their comparison with the proposed technique is being carried out. Vector estimation provided techniques that can offer better performance as compared to the other techniques from the same domain of signal processing.

By manipulating inter-frame correlations of a video sequence, de-noising performance can be made better. A novel approach of de-noising that finds its roots in the HMT vector extension [3] for the coefficients of wavelets has been proposed in this thesis. The use of term Vector illustrated the collection of wavelet coefficients in the neighborhood of the frame.

By approximating inter-frame correlations right from the noisy video data, Elastic sub band and time-based alterations are accomplished. It is suggested by the results that the methods of de-noising that are proposed and wavelet coefficient's vector estimation outperforms the currently available methods not only in terms of the noise reduction but also in terms of quality. The edges are preserved by VEWC de-noising.

6.2 Future Work

Although our proposed approach gives encouraging de-noising results, we believe that there is more room for improvement. This approach can be applied to high quality video. For example, a technique can also be developed that contain functions which are

more articulate, having better association with neighboring coefficients. Moreover, technique should also be doing a better representation of hierarchical dependence among the various levels of wavelet decomposition.

This approach can also be extended to multi-dimensional video de-noising. Since the model developed and the training algorithm apply to quad and higher dimensional trees that would be helpful in video Modeling for higher dimensions.

HM models do not only have the applicability to data in the form of wavelets but also can be utilized for modeling data from other multidimensional transforms and further signal representations.

At last, for the better accomplishment of performances, the proposed technique could be combined with other techniques and the combination must also be aiming at reducing the systems' complexity in terms of the computations that it would need to perform.

References

1. J. W. Woods and J, Kim, Motion Analysis and Image Sequence Processing, ch. 12. 1993.

2. M. 1. sezan, M. K. Ozkan, and S. V. Fogel, "Temporally adaptive filtering of noisy image sequences using a robust motion estimation algorithm," in ICASSP-91, pp. 2429-2432.

3. S. Fogel, "Estimation of velocity vector field from time-varying image sequences," CVGIP: Image Understanding, vol. 53, pp. 253—287, May 1991.

4. M. K. Ozkan, M. I. Sezan, and A. M. Tekalp, "Adaptive motion-compensated filtering of noisy image sequences," IEEE Trans. CSVT, vol. 3, pp. 277-290, Aug. 1993.

5. D. S. Taubman and M. W. Marcellin, JPEG 2000: Image Compression Fundamentals, Standards and Practice. Norwell, MA, USA: Kluwer Academic Publishers, 2001.

6. J. N. Bradley and C. M. Brislawn, "The wavelet scalar quantization compression standard for digital fingerprint images," in ISCAS, 1994, pp. 205–208.

7. H. Weng and K. M. Lau, "Wavelets, period doubling, and time-frequency localization with application to organization of convection over the tropical western Pacific," Journal of Atmospheric Science, vol. 51, p. 25232541, 1994.

8. B. Wang and Y. Wang, "Temporal structure of the southern oscillation as revealed by waveform and wavelet analysis," J. Climate, vol. 9, p. 15861598, 1996.

9. C. Torrence and G. P. Compo, "A practical guide to wavelet analysis," Bulletin of the American Meteorological Society, vol. 79, pp. 61–78, 1998.

10. S. Baliunas, P. Frick, D. Sokoloff, and W. Soon, "Time scales and trends in the central england temperature data (16591990): A wavelet analysis," Geophys. Res. Lett., vol. 24, p. 13511354, 1997.

11. E. Brannock, M. Weeks, and V. Rehder, "Detecting filopodia with wavelets," in Proceedings of the 2004 International Symposium on Circuits and Systems, May 2006.

12. E. Brannock and M. Weeks, "Edge detection using wavelets," in Proceedings of the 44th ACM SE 2006, March 2006, pp. 649–654.

13. M. S. Crouse, R. D. Nowak and R. G. Baraniuk, "Wavelet-based statistical signal processing using Hidden Markov Models", IEEE Trans. on Signal Processing, vol.46, 110.4, pp.886-9()2, Apr. 1998.

14. J. Romberg, H. Choi and R. G. Baraniuk, "Bayesian tree-structured image modeling using wavelet-domain Hidden Markov Models", IEEE Trans. on Image Processing, vol. 10, no. 7, pp. 1056-1068, July 2001.

15. J. M. Boyce, "Noise reduction of image sequences using adaptive motion compensated frame averagmg," in ICASSP-92, vol. 111, pp. 461-464.

16. J. C. Brailean, R. P. Kleihorst, S. Efstratiadis, A. K. Katsaggelos, and R. L. Lagendijk, "Noise reduction filters for dynamic image sequences: a review" , Proceedings of the IEEE, vol.83, no.9, pp. 1272-1292, Sept. 1995.

17. A. PiEurica and W. Philips, "Estimating probability of presence of a signal of interest in multiresolution single- and multiband image denoising" , to appear in IEEE Trans. Image Processing, Jan. 2005.

18. F. Dekeyser, P. Bouthemy and P. Perez, "Spatio-temporal Wiener filtering of image sequences using a parametric motion model", IEEE International Conference on Image Processing, vol. 1, pp. 208-211, Sept.2000

19. A. C. Kokaram, "On Missing Data Treatment for Degraded Video and Film Archives: A Survey and a new Bayesian approach" , IEEE Trans. on Image Processing, vol. 13, no. 3, pp.397-415, Mar. 2004.

20. R. Dugad and N. Ahuja, "Video denoising by combining Kalman and Wiener estimates", IEEE International Conference on Image Processing, vol.4, pp. 152-156, Oct. 1999.